

Original Research

SHMT as a Potential Therapeutic Target for Renal Cell Carcinoma

Yongli Situ¹, Juying Zhang^{1,4}, Wenyu Liao^{2,3}, Quanyan Liang^{1,4}, Lingling Lu¹, Qinying Xu¹, Jv Chen³, Xiaoyong Lu¹, Yongshi Cui¹, Zheng Shao^{1,*}, Li Deng^{1,*}¹Department of Parasitology, Guangdong Medical University, 524023 Zhanjiang, Guangdong, China²Department of Pharmacology, Guangdong Medical University, 524023 Zhanjiang, Guangdong, China³Department of Pharmacy, Affiliated Hospital of Guangdong Medical University, 524001 Zhanjiang, Guangdong, China⁴School of Medical Technology, Guangdong Medical University, 523808 Dongguan, Guangdong, China*Correspondence: shaozheng@gdmu.edu.cn (Zheng Shao); dengli@gdmu.edu.cn (Li Deng)

Academic Editor: Sukmook Lee

Submitted: 27 November 2022 Revised: 22 January 2023 Accepted: 10 February 2023 Published: 12 September 2023

Abstract

Background: Serine hydroxymethyltransferase (*SHMT*) is a serine-glycine-one-carbon metabolic enzyme in which *SHMT1* and *SHMT2* encode the cytoplasmic and mitochondrial isoenzymes, respectively. *SHMT1* and *SHMT2* are key players in cancer metabolic reprogramming, and thus are attractive targets for cancer therapy. However, the role of *SHMT* in patients with renal cell carcinoma (RCC) has not been fully elucidated. We aimed to systematically analyze the expression, gene regulatory network, prognostic value, and target prediction of *SHMT1* and *SHMT2* in patients with kidney chromophobe (KICH), kidney renal clear cell carcinoma (KIRC), and kidney renal papillary cell carcinoma (KIRP); elucidate the association between *SHMT* expression and RCC; and identify potential new targets for clinical RCC treatment. **Methods:** Several online databases were used for the analysis, including cBioPortal, TRRUST, GeneMANIA, GEPIA, Metascape, UALCAN, LinkedOmics, and TIMER. **Results:** *SHMT1* and *SHMT2* transcript levels were significantly down- and upregulated, respectively, in patients with KICH, KIRC, and KIRP, based on sample type, individual cancer stage, sex, and patient age. Compared to men, women with KIRC and KIRP showed significantly up- and downregulated *SHMT1* transcript levels, respectively. However, *SHMT2* transcript levels were significantly upregulated in the patients mentioned above. KIRC and KIRP patients with high *SHMT1* expression had longer survival periods than those with low *SHMT1* expression. In patients with KIRC, the findings were similar to those mentioned above. However, in KICH patients, the findings were the opposite regarding *SHMT2* expression. *SHMT1* versus *SHMT2* were altered by 9% versus 3% (n = 66 KICH patients), 4% versus 4% (n = 446 KIRC patients), and 6% versus 7% (n = 280 KIRP patients). *SHMT1* versus *SHMT2* promoter methylation levels were significantly up- and downregulated in patients with KIRP versus KIRC and KIRP, respectively. *SHMT1*, *SHMT2*, and their neighboring genes (NG) formed a complex network of interactions. The molecular functions of *SHMT1* and its NG in patients with KICH, KIRC, and KIRP, included clathrin adaptor, metalloendopeptidase, and GTPase regulator activities; lipid binding, active transmembrane transporter activity, and lipid transporter activity; and type I interferon receptor binding, integrin binding, and protein heterodimerization, respectively. Their respective Kyoto Encyclopedia of Genes and Genomes (KEGG) pathways were involved in lysosome activity, human immunodeficiency virus 1 infection, and endocytosis; coronavirus disease 2019 and neurodegeneration pathways (multiple diseases); and RIG-I-like receptor signaling pathway, cell cycle, and actin cytoskeleton regulation. The molecular functions of *SHMT2* and its NG in patients with KICH, KIRC, and KIRP included cell adhesion molecule binding and phospholipid binding; protein domain-specific binding, enzyme inhibitor activity, and endopeptidase activity; and hormone activity, integrin binding, and protein kinase regulator activity, respectively. For patients with KIRC versus KIRP, the KEGG pathways were involved in cAMP and calcium signaling pathways versus microRNAs (MiRNAs) in cancer cells and neuroactive ligand-receptor interactions, respectively. We identified the key transcription factors of *SHMT1* and its NG. **Conclusions:** *SHMT1* and *SHMT2* expression levels were different in patients with RCC. *SHMT1* and *SHMT2* may be potential therapeutic and prognostic biomarkers in these patients. Transcription factor (MYC, STAT1, PPARG, AR, SREBF2, and SP3) and miRNA (miR-17-5P, miR-422, miR-492, miR-137, miR-30A-3P, and miR-493) regulations may be important strategies for RCC treatment.

Keywords: *SHMT1*; *SHMT2*; renal cell carcinoma; target prediction; gene regulation network

1. Introduction

Renal cell carcinoma (RCC) is the most common kidney malignancy, accounting for approximately 90% of all renal malignancies [1]. An estimated 431,288 new RCC cases and 179,368 cancer-related deaths were recorded globally in 2020 [2]. The three main pathological types of RCC are kidney renal clear cell carcinoma (KIRC), kidney renal papillary cell carcinoma (KIRP), and kidney chromo-

phobe (KICH). KIRC is the most common type of RCC, accounting for 75–80% of RCC cases, followed by KIRP, accounting for 10–15% of cases [3]. In RCC, KICH accounts for approximately 4–5% of the cases [4]. RCC is the second most lethal urological malignancy [5]. In advanced RCC, the 5-year survival rate is only 11.7% [6]. Although alternative treatments exist, surgery is the gold standard for RCC treatment [7,8]. However, 20–40% of patients with



RCC experience relapse [9]. In addition, 90% of RCC recur within five years after surgery [10]. Cancer subtypes have different origins, histology, genetics, and epigenetic changes, and thus should be classified and treated as distinct cancers [11]. Hence, the systematic analysis of the targeted predictive and prognostic markers of patients with different RCC subtypes helps achieve precise treatment and improve the survival rates of these patients.

Serine hydroxymethyltransferase (*SHMT*) is a serine-glycine-one-carbon-metabolizing enzyme. *SHMT* catalyzes the conversion of serine to glycine, which transfers a one-carbon unit to tetrahydrofolate to produce 5,10-methylenetetrahydrofolate. This enzyme has cytoplasmic (*SHMT1*) and mitochondrial (*SHMT2*) isoforms [12], which are highly upregulated in cancer cells. Metabolic reprogramming mediated by *SHMT* isoenzymes is a hallmark of cancer that supports tumor growth, survival, and chemotherapy resistance [13]. Although normal cells rely on extracellular serine and glycine supplies, a substantial proportion of cancer patients are dependent to intracellular serine/glycine synthesis, thereby providing an attractive action target. Furthermore, one-carbon metabolism mediated by the folate co-factor promotes cancer growth and proliferation by supporting purine and pyrimidine biosynthesis, amino acid homeostasis, epigenetic maintenance, and redox defense [14–18]. Hence, modulating the expression of *SHMT* may be an effective cancer treatment strategy; this modulation is expected to be a target for blocking tumor progression and improving survival.

The role of *SHMT* in RCC pathogenesis is not well understood. Therefore, this study systematically analyzed the expression, gene regulatory network, prognostic value, and target prediction of *SHMT1* and *SHMT2* in patients with KICH, KIRC, and KIRP; elucidated the association between *SHMT* and RCC; and identified new potential targets for RCC therapy.

2. Materials and Methods

2.1 UALCAN Analysis

UALCAN (<http://ualcan.path.uab.edu/analysis.html>) is an online professional database for analyzing tumor gene expression and methylation levels. We used the UALCAN database to analyze the expression and methylation levels of *SHMT1* and *SHMT2* in healthy individuals and patients with KICH, KIRC, and KIRP. Furthermore, we used the Student's *t*-test for comparative analysis, and the difference was considered significant at a *p*-value < 0.05 [19,20].

2.2 GEPIA Analysis

Gene Expression Profiling (GEPIA) (<http://gepia.canc er-pku.cn/index.html>) is a free online platform for analyzing the correlation between gene expression levels and the pathological tumor stage and prognostic value. We used the GEPIA database to analyze the correlation between pathological tumor stage and the prognostic value of *SHMT1* and

SHMT2 expression levels in patients with KICH, KIRC, and KIRP. Comparative analysis was performed using Student's *t*-tests, with a *p*-value less than 0.05 considered significant [19,20].

2.3 cBioPortal Analysis

cBioPortal (<http://cbioportal.org>) is an online professional database used to analyze genetic alterations in tumors. We used the cBioPortal database to analyze genetic alterations in *SHMT1*, *SHMT2*, and their neighboring genes (NG). A total of 66, 446, and 280 KICH, KIRC, and KIRP samples were analyzed, respectively, and mRNA expression z-scores were obtained relative to all samples (log RNA Seq V2 RSEM) using a z-score threshold of ± 2.0 [19,20].

2.4 STRING Analysis

STRING (<https://string-db.org/cgi/input.pl>) is an online professional database for analyzing protein-protein interactions (PPI). We used the STRING database to build a low-confidence level (0.150) PPI network and screening criteria for species defined as humans. Finally, K-means cluster analysis was performed on *SHMT1*, *SHMT2*, and their NG [19,20].

2.5 GeneMANIA Analysis

GeneMANIA (<http://www.genemania.org>) is a free professional tool for analyzing gene interactions. We used the GeneMANIA database to explore the interactions between *SHMT1*, *SHMT2*, and their altered NG [19,20].

2.6 Metascape Analysis

Metascape (<https://metascape.org>) is a professional-free tool for analyzing gene ontology (GO) functions and the Kyoto Encyclopedia of Genes and Genomes (KEGG) pathway enrichment. We used the Metascape database to analyze the GO function and KEGG pathway enrichment of *SHMT1*, *SHMT2*, and their altered NG in patients with KICH, KIRC, and KIRP [19,20].

2.7 TRRUST Analysis

TRRUST (<https://www.grnpedia.org/trrust/>) is an online professional database that analyzes transcriptional gene regulators. We used the TRRUST database to analyze the transcriptional regulators of *SHMT1*, *SHMT2*, and their altered NG in patients with RCC.

2.8 LinkedOmics Analysis

LinkedOmics (<http://www.linkedomics.org/>) is a free online platform for analyzing microRNA (miRNA) target enrichment and differentially expressed genes associated with tumor genes. We used the LinkedOmics database to analyze the miRNA target enrichment and differentially expressed genes associated with *SHMT1* and *SHMT2* [19,20].

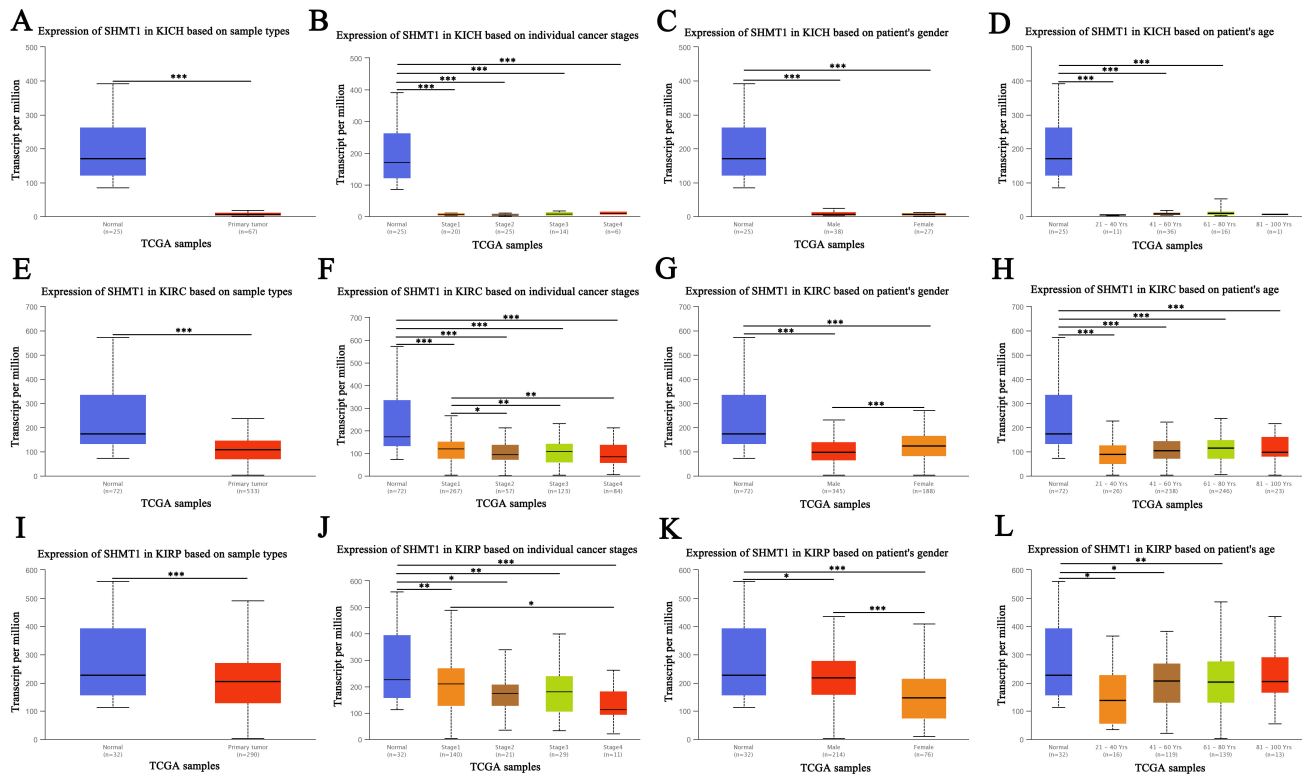


Fig. 1. Expression of *SHMT1* in RCC (UALCAN). (A) The expression of *SHMT1* in KICH based on sample types. (B) The expression of *SHMT1* in KICH based on individual cancer stage. (C) The expression of *SHMT1* in KICH based on patient's gender. (D) The expression of *SHMT1* in KICH based on patient's age. (E) The expression of *SHMT1* in KIRC based on sample types. (F) The expression of *SHMT1* in KIRC based on individual cancer stage. (G) The expression of *SHMT1* in KIRC based on patient's gender. (H) The expression of *SHMT1* in KIRC based on patient's age. (I) The expression of *SHMT1* in KIRP based on sample types. (J) The expression of *SHMT1* in KIRP based on individual cancer stage. (K) The expression of *SHMT1* in KIRP based on patient's gender. (L) The expression of *SHMT1* in KIRP based on patient's age; Data are expressed as mean \pm SE. * $p < 0.05$; ** $p < 0.01$; *** $p < 0.001$.

2.9 TIMER Analysis

TIMER (<https://cistrome.shinyapps.io/timer/>) is a specialized database for systematically analyzing tumor genes associated with infiltrating immune cells. We used the TIMER database to analyze the correlation between *SHMT1* and *SHMT2* expression and immune cell infiltration levels [19,20].

3. Results

3.1 *SHMT* Expression in RCC

We compared the *SHMT1* and *SHMT2* expression levels based on sample type, individual cancer stage, sex, and patient age among patients with RCC. Results showed that *SHMT1* transcript levels were significantly downregulated in patients with KICH, KIRC, and KIRP, based on sample type, individual cancer stage, sex, and patient age ($p < 0.05$; Fig. 1). The transcript level of *SHMT1* in stage 4 cancer was significantly lower than in stage 1 among patients with KIRC and KIRP ($p < 0.05$; Fig. 1F,J). In patients with KIRC, *SHMT1* transcript levels were significantly upregulated in females compared to males ($p < 0.001$; Fig. 1G). However, *SHMT1* transcript levels in patients with KIRP

were significantly downregulated in females compared to that in males ($p < 0.001$; Fig. 1K). In addition, results indicated that *SHMT2* transcript levels were significantly upregulated in patients with KICH, KIRC, and KIRP, based on sample type, individual cancer stage, sex, and patient age ($p < 0.05$; Fig. 2). In patients with KIRP, *SHMT2* transcript levels were significantly upregulated in females compared to that in males ($p < 0.05$; Fig. 2K).

Moreover, we evaluated the correlation between the differential expression levels of *SHMT1* and *SHMT2* and the pathological stage of RCC. A significant correlation was found between the expression of *SHMT1* ($p = 0.0142$; Fig. 3B) and pathological stage of KIRC. The expression of *SHMT1* ($p = 0.00326$; Fig. 3C), *SHMT2* ($p = 7.32 \times 10^{-8}$; Fig. 3F), and the pathological stage of KIRP also had a significant correlation. Moreover, results showed a significant correlation between the expression of *SHMT2* ($p = 0.000135$; Fig. 3D) and pathological stage of KICH.

Finally, the GEPIA database was used to assess the prognostic value of *SHMT1* and *SHMT2* expression in patients with RCC. Results indicated that patients with KIRC, and those with KIRP, with high *SHMT1* expression had a

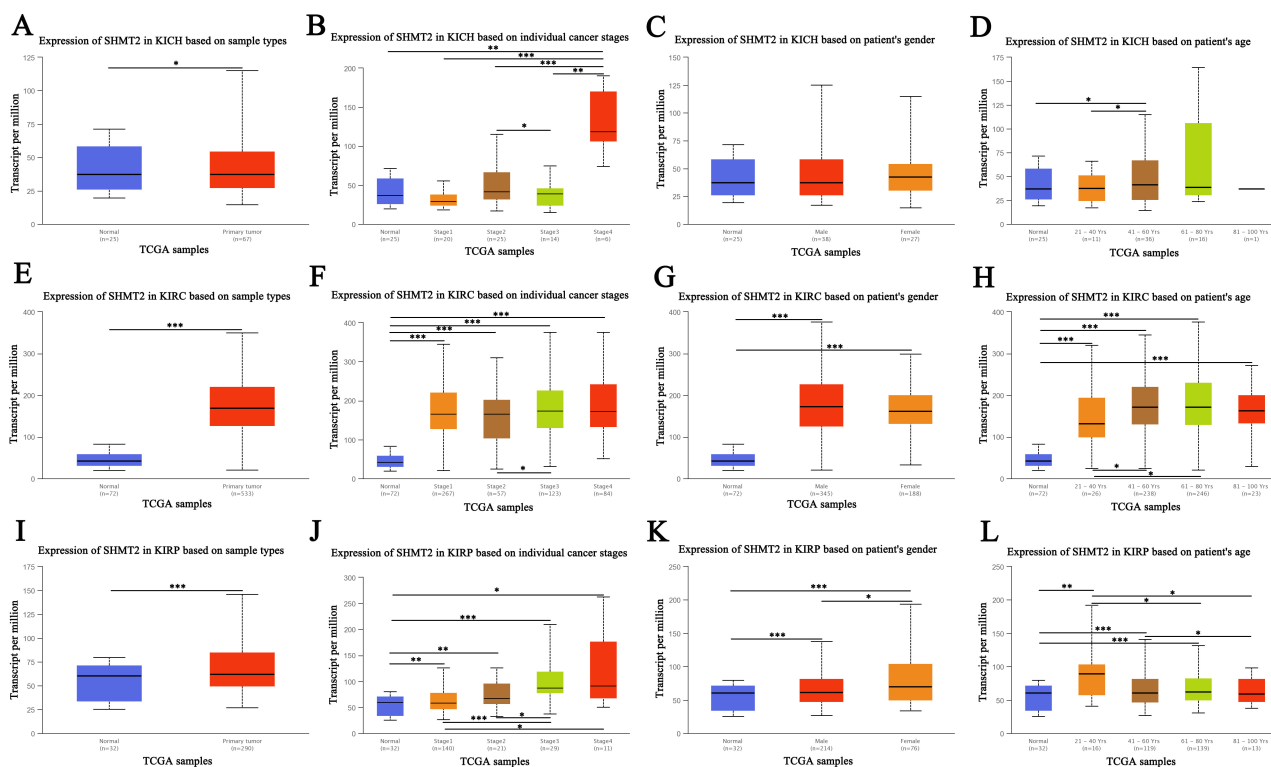


Fig. 2. Expression of *SHMT2* in renal cell carcinoma (RCC) (UALCAN). (A) The expression of *SHMT2* in KICH based on sample types. (B) The expression of *SHMT2* in KICH based on individual cancer stage. (C) The expression of *SHMT2* in KICH based on patient's gender. (D) The expression of *SHMT2* in KICH based on patient's age. (E) The expression of *SHMT2* in KIRC based on sample types. (F) The expression of *SHMT2* in KIRC based on individual cancer stage. (G) The expression of *SHMT2* in KIRC based on patient's gender. (H) The expression of *SHMT2* in KIRC based on patient's age. (I) The expression of *SHMT2* in KIRP based on sample types. (J) The expression of *SHMT2* in KIRP based on individual cancer stage. (K) The expression of *SHMT2* in KIRP based on patient's gender. (L) The expression of *SHMT2* in KIRP based on patient's age; Data are expressed as mean \pm SE. * $p < 0.05$; ** $p < 0.01$; *** $p < 0.001$.

longer overall and disease-free survival rate than those with low *SHMT1* expression ($p < 0.05$; Fig. 4C–F). In contrast, patients with KICH with low *SHMT2* expression had longer overall and disease-free survival times than those with high *SHMT2* expression ($p < 0.05$; Fig. 5A,B). However, patients with KIRC with high *SHMT2* expression had longer overall survival times than those with low *SHMT2* expression ($p < 0.05$; Fig. 5C).

3.2 Genetic Alteration and Promoter Methylation of *SHMT* in RCC

The genetic alterations in *SHMT1* and *SHMT2* were assessed in 66, 446, and 280 patients with KICH, KIRC, and KIRP, respectively, using the TCGA database. Results indicated that *SHMT1* expression was altered by 9% in patients with KICH, and the types of genetic alterations mainly included high- and low RNA levels (Fig. 6A). In addition, *SHMT1* and *SHMT2* expression levels were altered by 4% in patients with KIRC. The types of genetic alterations mainly included missense and truncating mutations as well as high- and low RNA levels (Fig. 6E and Fig. 7E). Meanwhile, among patients with KIRP the *SHMT1* expression was altered by 6%, and the types of genetic alterations

mainly included missense mutations, deep deletions, and low RNA levels (Fig. 6J). *SHMT2* expression was altered by 3% in patients with KICH, and the type of genetic alteration mainly included high RNA levels (Fig. 7A). Meanwhile, the expression of *SHMT2* was altered by 7% among patients with KIRP, and the types of genetic alterations mainly included missense mutations, amplification, and high and low RNA levels (Fig. 7J).

Subsequently, we assessed the promoter methylation levels of *SHMT1* and *SHMT2* in patients with RCC using the UALCAN database. Results indicate that *SHMT1* promoter methylation levels were significantly upregulated in patients with KIRP, based on sample type, individual cancer stage (stages 1 and 3), and patient age (41–60 years and 61–80 years) ($p < 0.05$; Fig. 6K,L,N). *SHMT1* promoter methylation levels were significantly upregulated in male patients with KIRP ($p < 0.001$; Fig. 6M). However, *SHMT2* promoter methylation levels were significantly downregulated in patients with KIRC and KIRP based on sample type, individual cancer stage, sex, and patient age ($p < 0.05$; Fig. 7F–N).

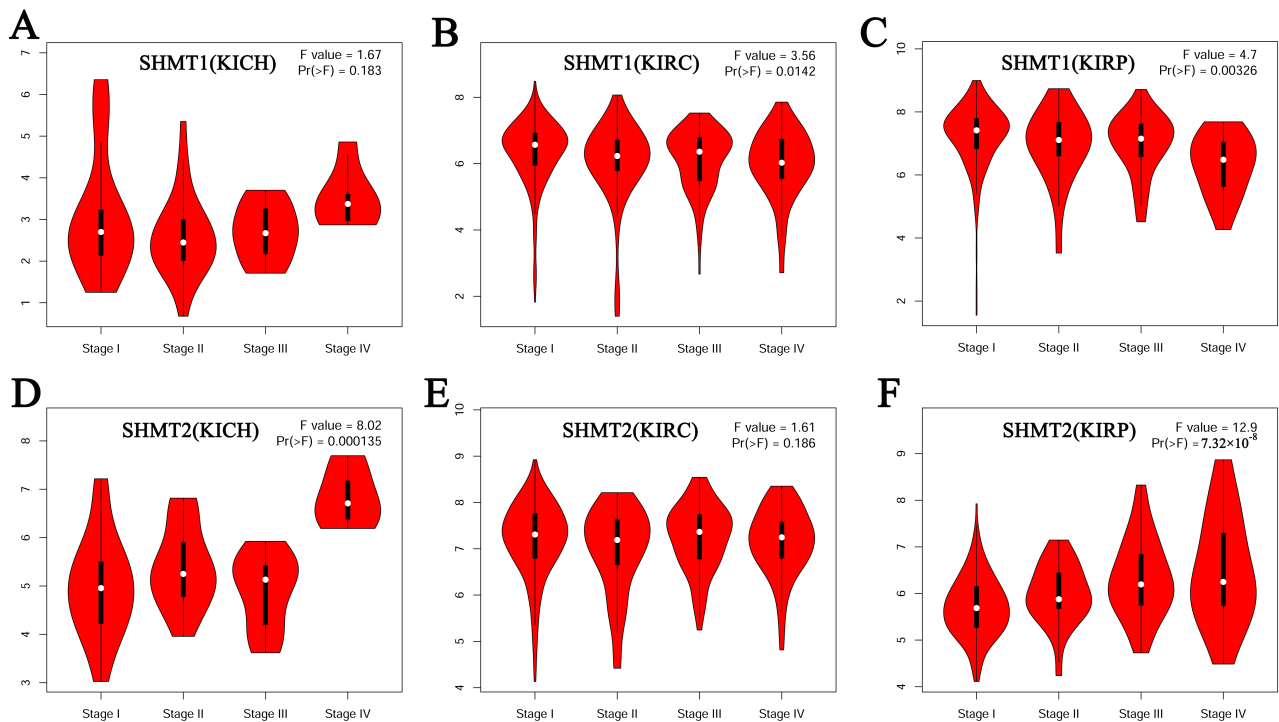


Fig. 3. Correlation between the expression of SHMT and the pathological stage of RCC (GEPIA). (A) *SHMT1* in patients with KICH. (B) *SHMT1* in patients with KIRC. (C) *SHMT1* in patients with KIRP. (D) *SHMT2* in patients with KICH. (E) *SHMT2* in patients with KIRC. (F) *SHMT2* in patients with KIRP.

3.3 NG Alteration and SHMT Interaction Network in RCC

We evaluated alterations in the NG of *SHMT1* and *SHMT2* in RCC using the cBioPortal database. Results showed gene alteration frequencies $\geq 16.67\%$, $\geq 16.67\%$, and $\geq 11.76\%$ for the 50 most frequently altered NG of *SHMT1* in patients with KICH, KIRC, and KIRP, respectively (Tables 1,2,3). Furthermore, in patients with KICH, KIRC, and KIRP, the 50 most frequently altered NG of *SHMT2* showed 100.00%, $\geq 15.79\%$, and $\geq 10.00\%$, respectively (Tables 4,5,6). In patients with KICH, KIRC, and KIRP, the most frequently altered NG of *SHMT1* were *AP5Z1* (33.33%), *MUC16* (20.00%), and *STAG2* (23.53%), respectively (Tables 1,2,3). However, *AARD* (100.00%), *PAPPA2* (31.58%), and *CDKN2A* (55.00%) were the most frequently altered NG of *SHMT2* among patients with KICH, KIRC, and KIRP, respectively (Tables 4,5,6).

We further evaluated the potential interactions between *SHMT1*, *SHMT2*, and their NG. Results indicated that 42 nodes, 146 edges, and 3 clusters were obtained in the constructed PPI network of *SHMT1* and its NG among patients with KICH (Fig. 8A). *SHMT1* and its NG were linked to a complex interaction network (71 genes and 267 edges) through physical interactions, co-expression, pathways, shared protein domains, and predictions (Fig. 8B). Furthermore, we found that 40 nodes, 106 edges, and 3 clusters were obtained in the constructed PPI network of *SHMT1* and its NG among patients with KIRC (Fig. 8C).

SHMT1 and its NG were linked to a complex interaction network (70 genes and 389 edges) through co-expression, pathway, genetic interactions, co-localization, and shared protein domains (Fig. 8D). Furthermore, 44 nodes, 198 edges, and 3 clusters were obtained in the constructed PPI network of *SHMT1* and its NG among patients with KIRP (Fig. 8E). *SHMT1* and its NG were linked to a complex interaction network (71 genes and 361 edges) through co-expression, physical interactions, shared protein domains, co-localization, and prediction (Fig. 8F). Conversely, 34 nodes, 206 edges, and 3 clusters were obtained in the constructed PPI network of *SHMT2* and its NG in KICH (Fig. 9A). *SHMT2* and its NG were linked to a complex interaction network (56 genes and 154 edges) through co-expression, physical interactions, and shared protein domains (Fig. 9B). In addition, 38 nodes, 146 edges, and 3 clusters were obtained in the constructed PPI network of *SHMT2* and its NG in KIRC (Fig. 9C). *SHMT2* and its NG were linked to a complex interaction network (71 genes and 151 edges) through co-expression, co-localization, physical interactions, shared protein domains, and prediction (Fig. 9D). A total of 43 nodes, 148 edges, and 3 clusters were obtained in the constructed PPI network of *SHMT2* and its NG among patients with KIRP (Fig. 9E). *SHMT2* and its NG were linked to a complex interaction network (71 genes and 219 edges) through co-expression, physical interactions, co-localization, shared protein domains, and prediction (Fig. 9F).

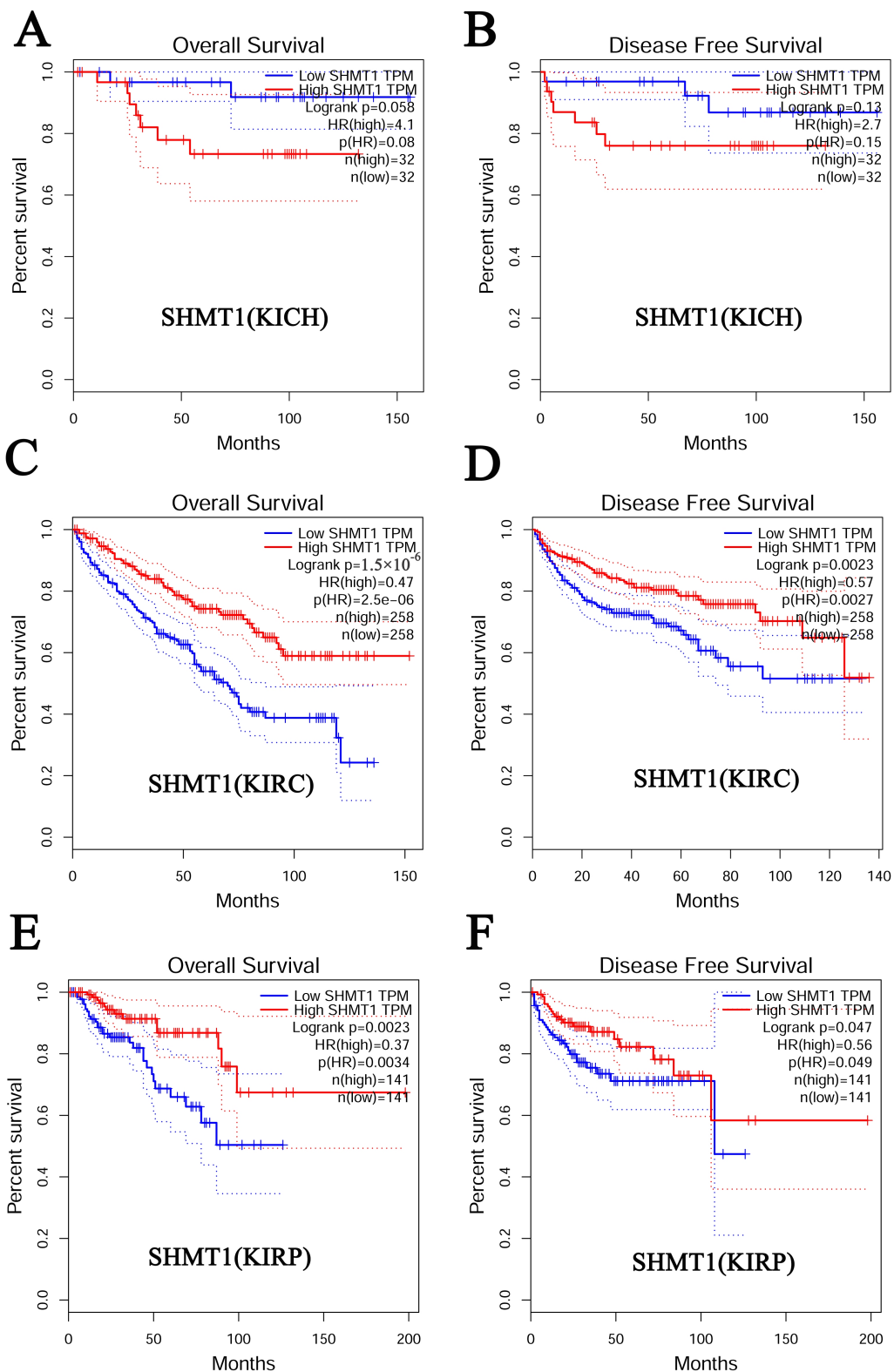


Fig. 4. Prognostic value of *SHMT1* in RCC (GEPIA). (A) The overall survival curve for patients with KICH based on *SHMT1* expression levels. (B) The disease-free survival curve for patients with KICH based on *SHMT1* expression levels. (C) The overall survival curve for patients with KIRC based on *SHMT1* expression levels. (D) The disease-free survival curve for patients with KIRC based on *SHMT1* expression levels. (E) The overall survival curve for patients with KIRP based on *SHMT1* expression levels. (F) The disease-free survival curve for patients with KIRP based on *SHMT1* expression levels.

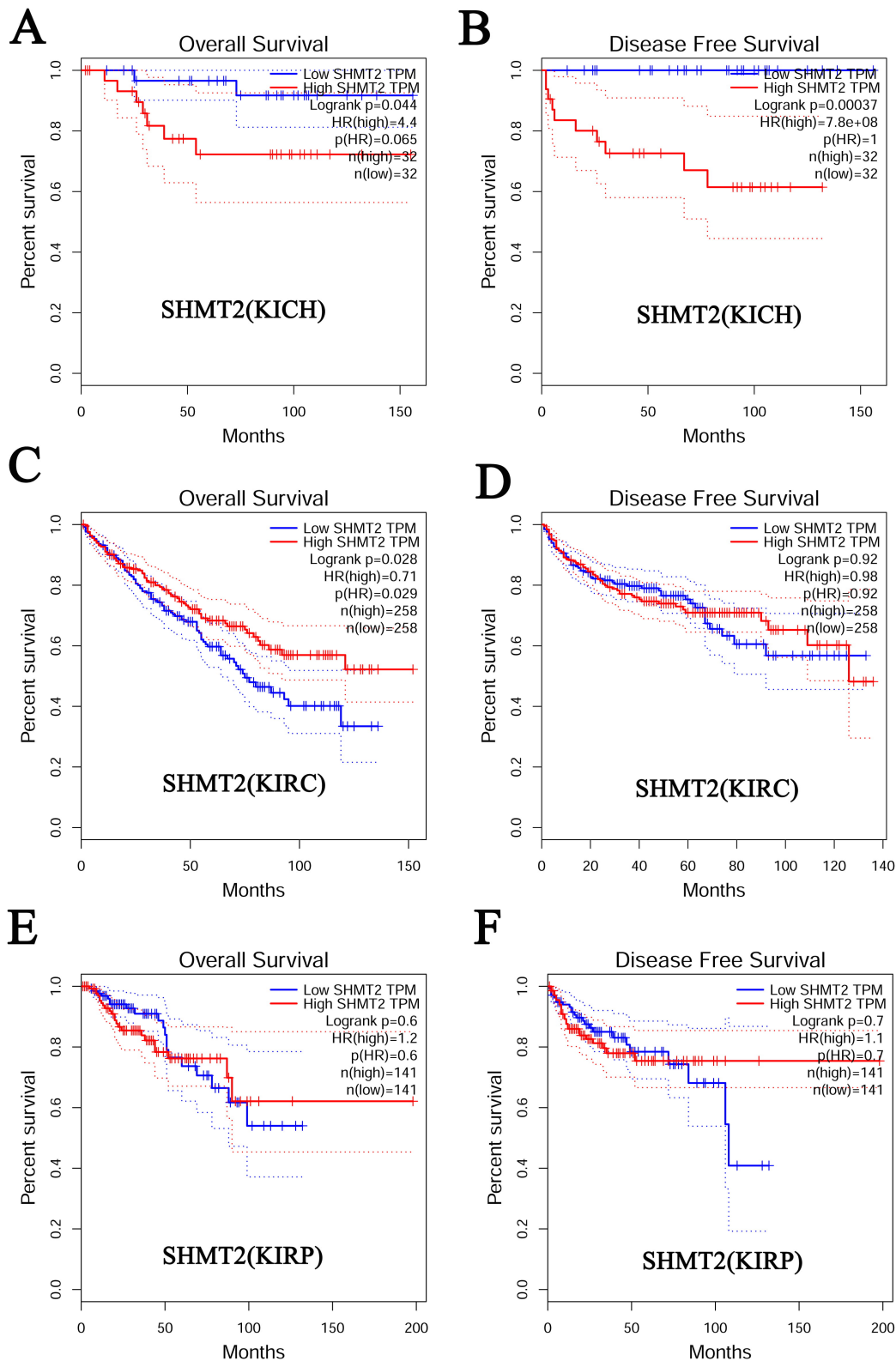


Fig. 5. Prognostic value of *SHMT2* in RCC (GEPIA). (A) The overall survival curve for patients with KICH based on *SHMT2* expression levels. (B) The disease-free survival curve for patients with KICH based on *SHMT2* expression levels. (C) The overall survival curve for patients with KIRC based on *SHMT2* expression levels. (D) The disease-free survival curve for patients with KIRC based on *SHMT2* expression levels. (E) The overall survival curve for patients with KIRP based on *SHMT2* expression levels. (F) The disease-free survival curve for patients with KIRP based on *SHMT2* expression levels.

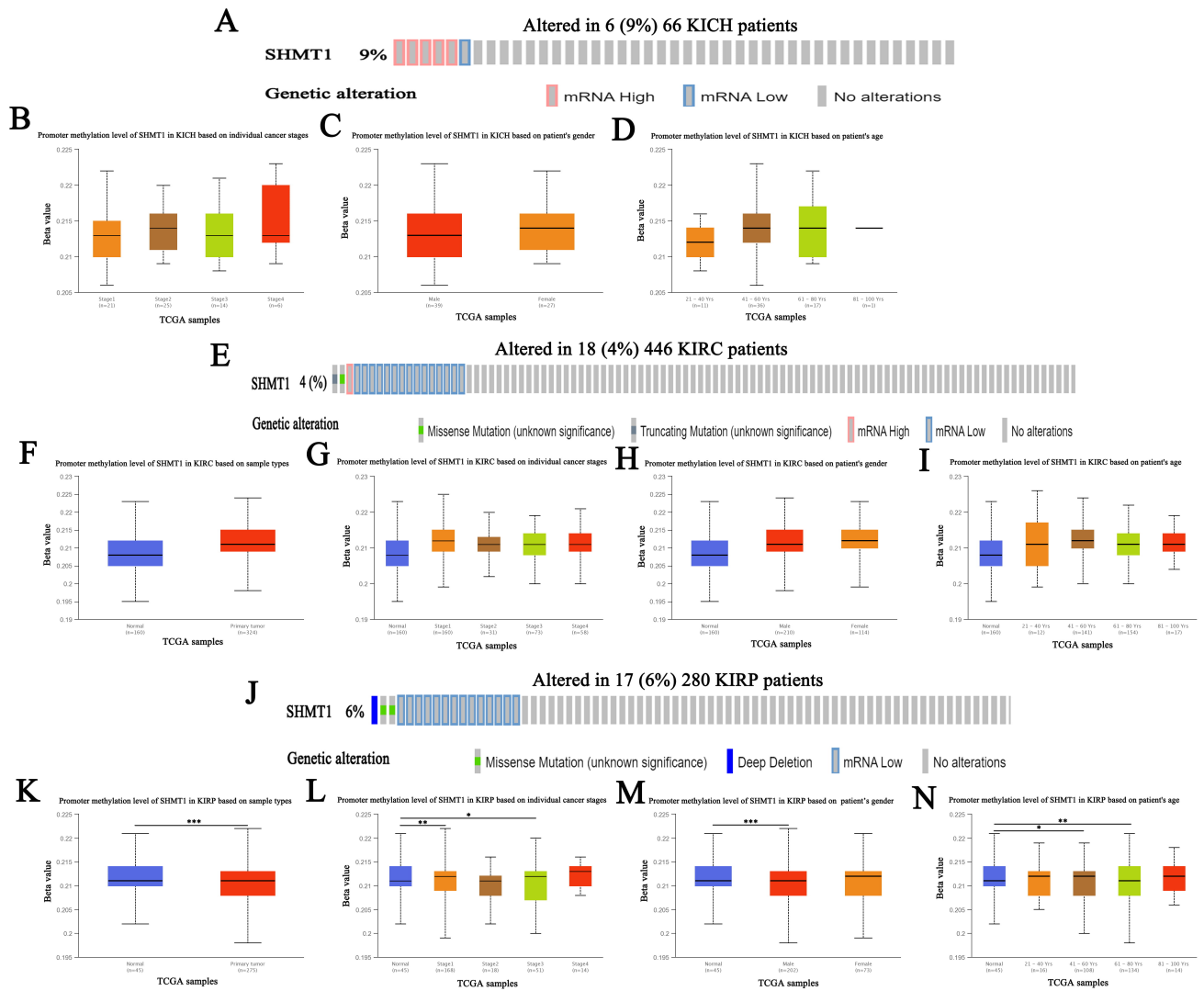


Fig. 6. Genetic alteration and promoter methylation of *SHMT1* in RCC (UALCAN). (A) Genetic alteration of *SHMT1* in patients with KICH. (B) Promoter methylation of *SHMT1* in KICH based on individual cancer stage. (C) Promoter methylation of *SHMT1* in KICH based on patient's gender. (D) Promoter methylation of *SHMT1* in KICH based on patient's age. (E) Genetic alteration of *SHMT1* in patients with KIRC. (F) Promoter methylation of *SHMT1* in KIRC based on sample types. (G) Promoter methylation of *SHMT1* in KIRC based on individual cancer stage. (H) Promoter methylation of *SHMT1* in KIRC based on patient's gender. (I) Promoter methylation of *SHMT1* in KIRC based on patient's age. (J) Genetic alteration of *SHMT1* in patients with KIRP. (K) Promoter methylation of *SHMT1* in KIRP based on sample types. (L) Promoter methylation of *SHMT1* in KIRP based on individual cancer stage. (M) Promoter methylation of *SHMT1* in KIRP based on patient's gender. (N) Promoter methylation of *SHMT1* in KIRP based on patient's age; Data are expressed as mean \pm SE. * $p < 0.05$; ** $p < 0.01$; *** $p < 0.001$.

3.4 GO and KEGG Pathway Enrichment Analyses

We further performed GO and KEGG pathway enrichment analyses of *SHMT1*, *SHMT2*, and their top 50 altered NG in patients with RCC using the Metascape database. Results indicated that biological processes related to *SHMT1* and its NG among patients with KICH mainly included cardiac muscle cell development, pyrimidine-containing compound metabolic processes, and multicellular organismal signaling (Fig. 10A). Their cellular components included the AP-type membrane coat adaptor complex, anchored membrane component, and synaptic mem-

brane (Fig. 10B). Clathrin adaptor-, metalloendopeptidase-, and GTPase regulator activities were involved to their molecular functions (Fig. 10C). KEGG pathway analysis revealed that lysosome activity, human immunodeficiency virus 1 infection, and endocytosis were enriched (Fig. 10D). However, our results showed that synapse assembly, canonical Wnt signaling pathway regulation, and myeloid cell differentiation regulation were the biological processes related to *SHMT1* and its NG among patients with KIRC (Fig. 10E). Neuronal cell bodies, sites of polarized growth, and extrinsic membrane components were related to their

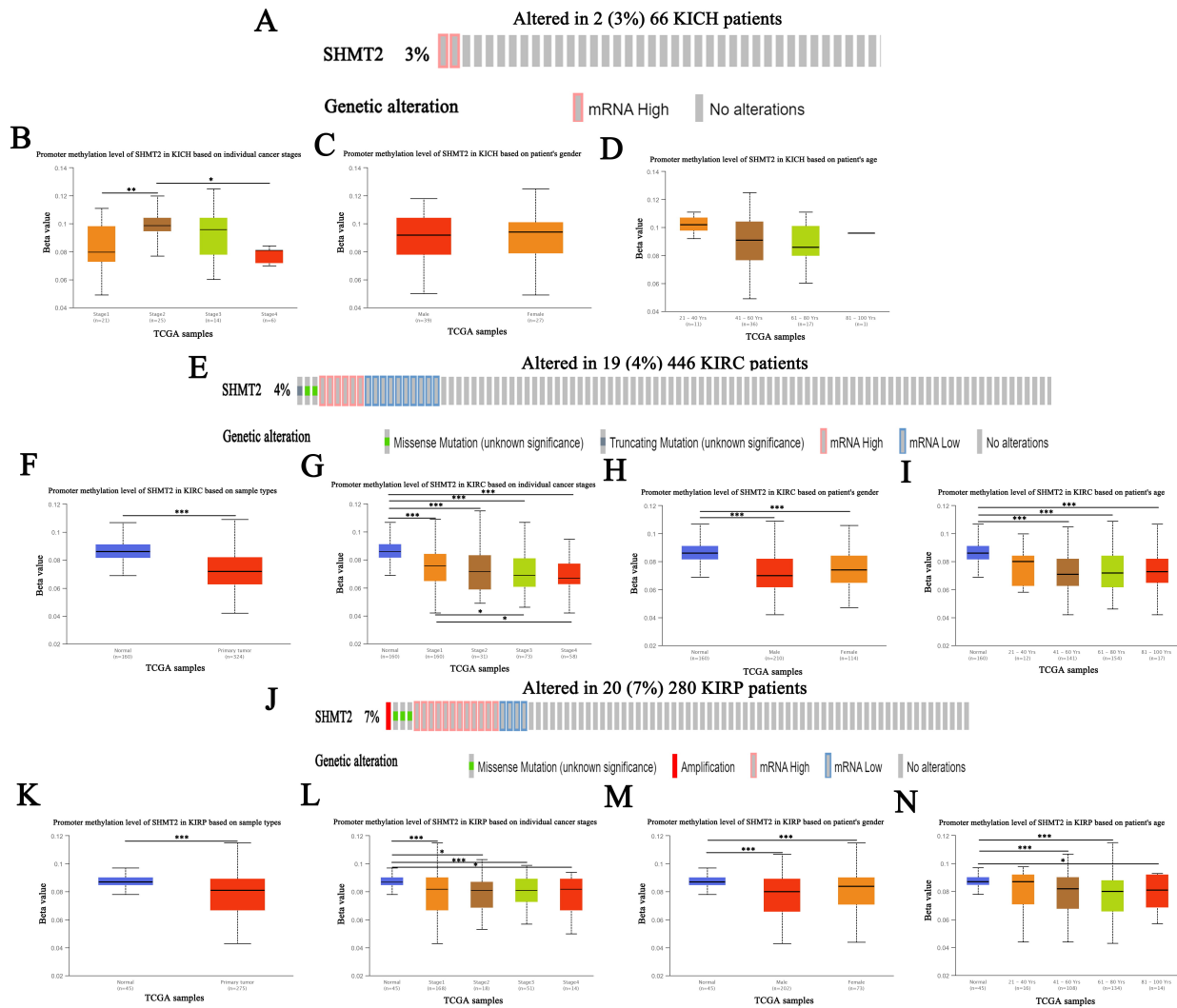


Fig. 7. Genetic alteration and promoter methylation of *SHMT2* in RCC (UALCAN). (A) Genetic alteration of *SHMT2* in patients with KICH. (B) Promoter methylation of *SHMT2* in KICH based on individual cancer stage. (C) Promoter methylation of *SHMT2* in KICH based on patient's gender. (D) Promoter methylation of *SHMT2* in KICH based on patient's age. (E) Genetic alteration of *SHMT2* in patients with KIRC. (F) Promoter methylation of *SHMT2* in KIRC based on sample types. (G) Promoter methylation of *SHMT2* in KIRC based on individual cancer stage. (H) Promoter methylation of *SHMT2* in KIRC based on patient's gender. (I) Promoter methylation of *SHMT2* in KIRC based on patient's age. (J) Genetic alteration of *SHMT2* in patients with KIRP. (K) Promoter methylation of *SHMT2* in KIRP based on sample types. (L) Promoter methylation of *SHMT2* in KIRP based on individual cancer stage. (M) Promoter methylation of *SHMT2* in KIRP based on patient's gender. (N) Promoter methylation of *SHMT2* in KIRP based on patient's age; Data are expressed as mean \pm SE. * $p < 0.05$; ** $p < 0.01$; *** $p < 0.001$.

cellular components (Fig. 10F). Lipid binding and active transmembrane transporter- and lipid transporter activity were related to their main molecular functions (Fig. 10G). KEGG pathway analysis revealed that *SHMT1* and its NG were associated with the coronavirus disease 2019 and pathways of neurodegeneration (Fig. 10H). Furthermore, biological processes related to *SHMT1* and its NG among patients with KIRP mainly included a positive regulation of peptidyl-serine phosphorylation of the STAT protein, nucleocytoplasmic transport, and cellular response to hypoxia (Fig. 10I). The cellular components were the external side of the plasma membrane, axon, and chromosomal region

(Fig. 10J). Type I interferon receptor binding, integrin binding, and protein heterodimerization were associated with their main molecular functions (Fig. 10K). RIG-I-like receptor signaling pathway, cell cycle, and actin cytoskeleton regulation were enriched according to the KEGG pathway analysis (Fig. 10L).

The biological processes related to *SHMT2* and its NG among patients with KICH mainly included plasma membrane organization, cell-cell junction organization, and positive regulation of organelle organization (Fig. 11A). Their cellular components included the ubiquitin ligase complex, chromosomal region, and mitochondrial membrane

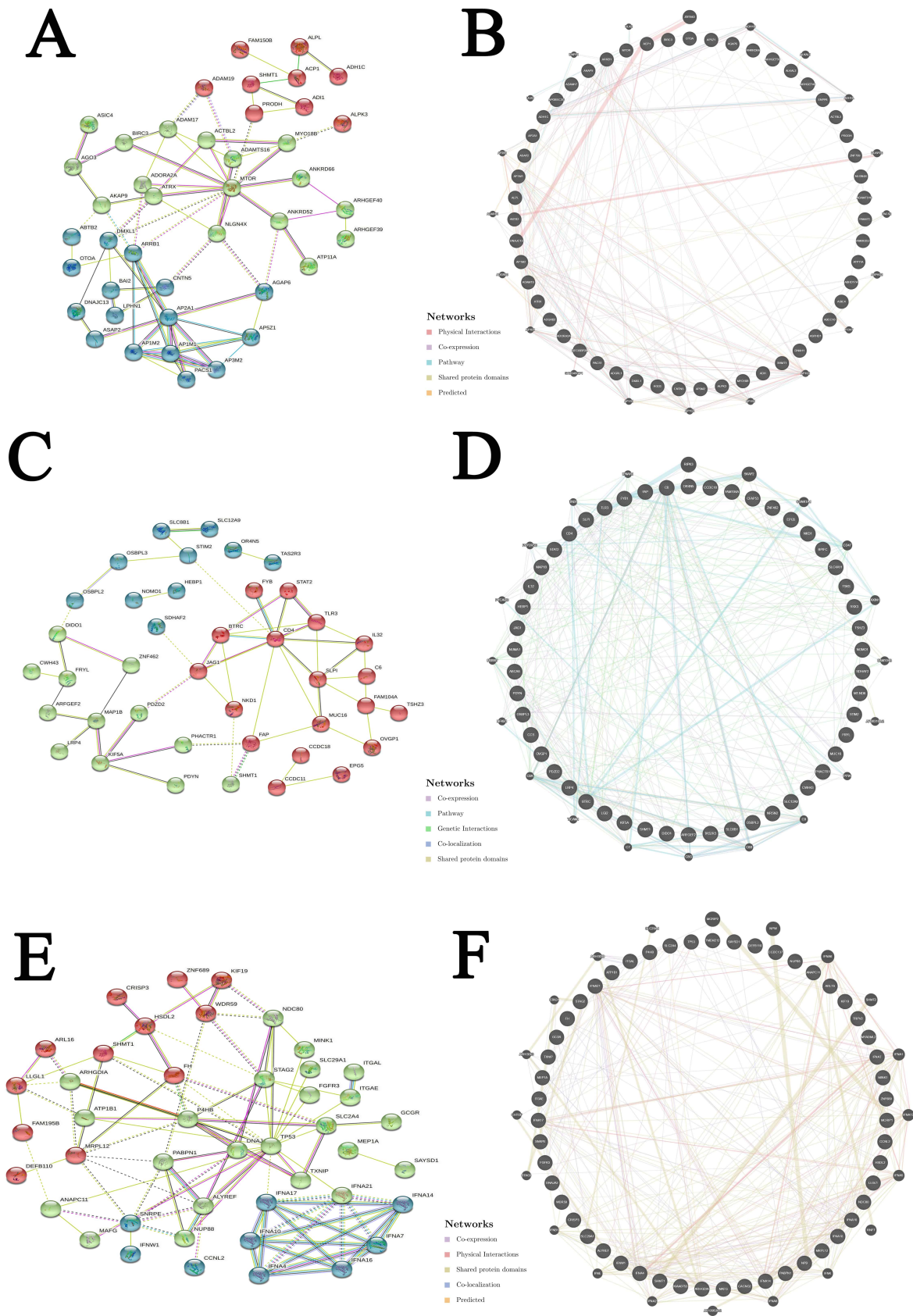


Fig. 8. Interaction analyses of *SHMT1* and their NG in RCC (STRING and GeneMANIA). (A) PPI network of *SHMT1* and its NG in KICH. (B) Network analyses of *SHMT1* and its NG in KICH. (C) PPI network of *SHMT1* and its NG in KIRC. (D) Network analyses of *SHMT1* and its NG in KIRC. (E) PPI network of *SHMT1* and its NG in KIRP. (F) Network analyses of *SHMT1* and its NG in KIRP.

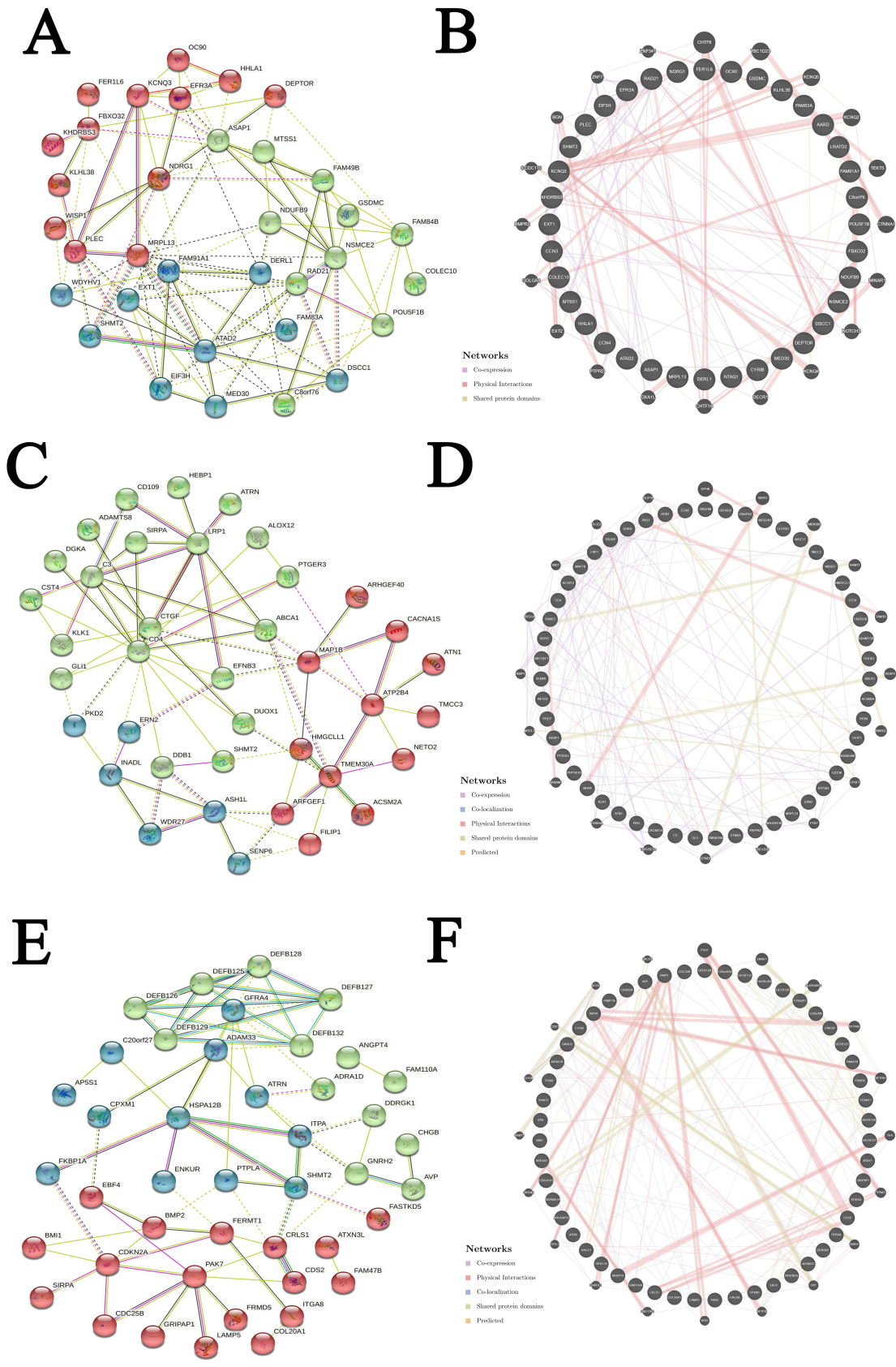


Fig. 9. Interaction analyses of *SHMT2* and their NG in RCC (STRING and GeneMANIA). (A) PPI network of *SHMT2* and its NG in KICH. (B) Network analyses of *SHMT2* and its NG in KICH. (C) PPI network of *SHMT2* and its NG in KIRC. (D) Network analyses of *SHMT2* and its NG in KIRC. (E) PPI network of *SHMT2* and its NG in KIRP. (F) Network analyses of *SHMT2* and its NG in KIRP.

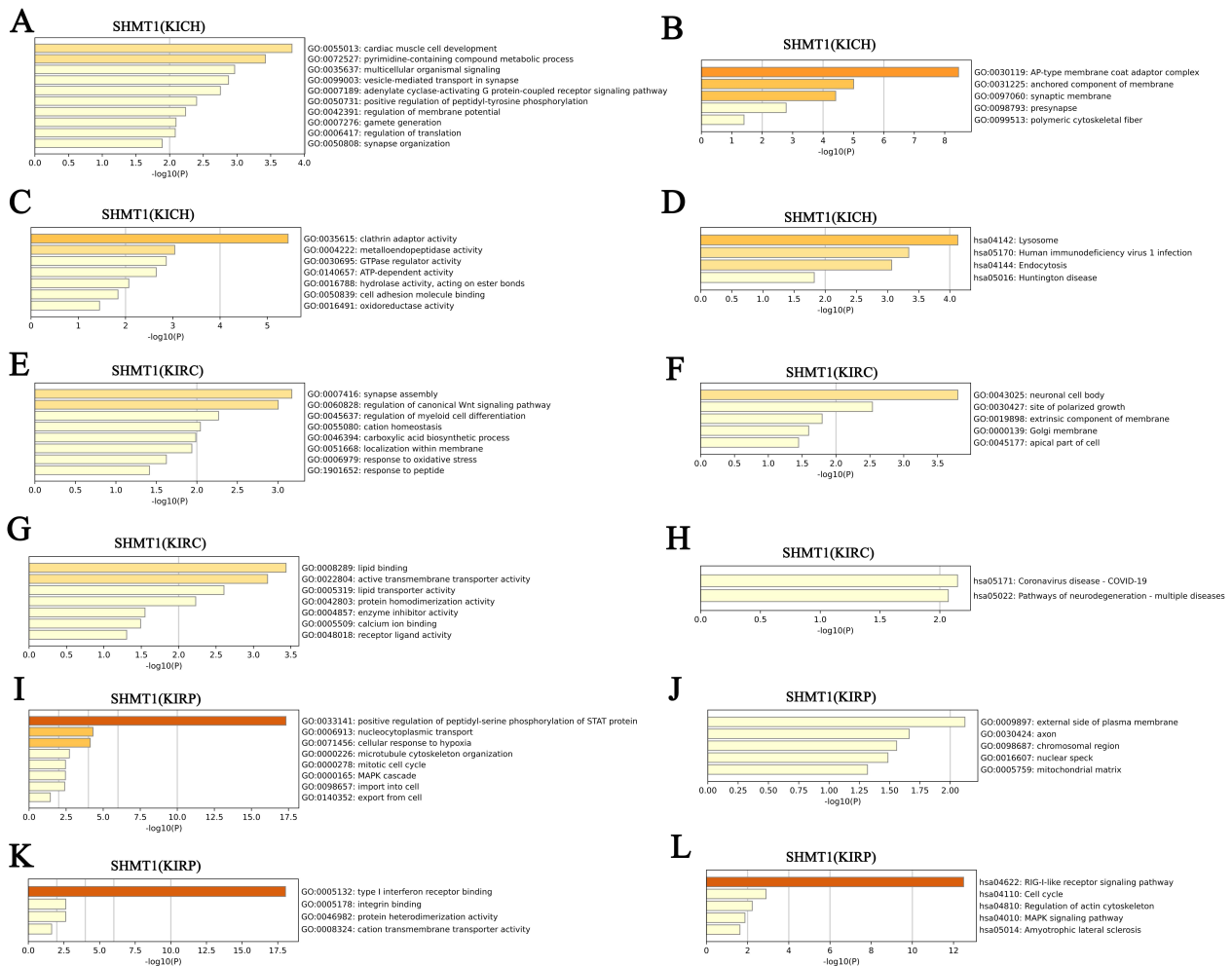


Fig. 10. GO function and KEGG pathways enrichment analyses of *SHMT1* and their NG in RCC (Metascape). (A) Biological processes of *SHMT1* and its NG in KICH. (B) Cellular components of *SHMT1* and its NG in KICH. (C) Molecular functions of *SHMT1* and its NG in KICH. (D) KEGG pathway analysis of *SHMT1* and its NG in KICH. (E) Biological processes of *SHMT1* and its NG in KIRC. (F) Cellular components of *SHMT1* and its NG in KIRC. (G) Molecular functions of *SHMT1* and its NG in KIRC. (H) KEGG pathway analysis of *SHMT1* and its NG in KIRC. (I) Biological processes of *SHMT1* and its NG in KIRP. (J) Cellular components of *SHMT1* and its NG in KIRP. (K) Molecular functions of *SHMT1* and its NG in KIRP. (L) KEGG pathway analysis of *SHMT1* and its NG in KIRP.

(Fig. 11B). Cell adhesion molecule and phospholipid bindings were involved to their molecular functions (Fig. 11C). However, we found that calcium ion transmembrane import into the cytosol, positive regulation of lipid localization, and regulation of acute inflammatory response were biological processes associated to *SHMT2* and its NG among patients with KIRC (Fig. 11D). The apical plasma membrane, perinuclear region of the cytoplasm, and sarcolemma were related to their cellular components (Fig. 11E). Protein domain-specific binding, enzyme inhibitor activity, and endopeptidase activity were associated to their main molecular functions (Fig. 11F). KEGG pathway analysis revealed that *SHMT2* and its NG were associated with cAMP and calcium signaling pathways (Fig. 11G). Furthermore, biological processes related to *SHMT2* and its NG among patients with KIRP mainly included the regulation of the transform-

ing growth factor-beta receptor signaling pathway, defense response to Gram-negative bacteria, and positive binding regulation (Fig. 11H). Their cellular components included the leading-edge membrane, extrinsic membrane component, and spindle (Fig. 11I). Hormone activity, integrin, and protein kinase regulatory activity was related to their main molecular functions (Fig. 11J). MiRNAs involved in cancer and neuroactive ligand-receptor interactions were enriched according to KEGG pathway analysis (Fig. 11K).

3.5 Transcription Factor and miRNA Targets of *SHMT1* in RCC

We used the TRRUST database to analyze the key regulatory factors of *SHMT1* and *SHMT2* in patients with RCC. We found that MYC was the critical transcription factor of *SHMT1* and its NG among patients with KICH ($p < 0.05$)

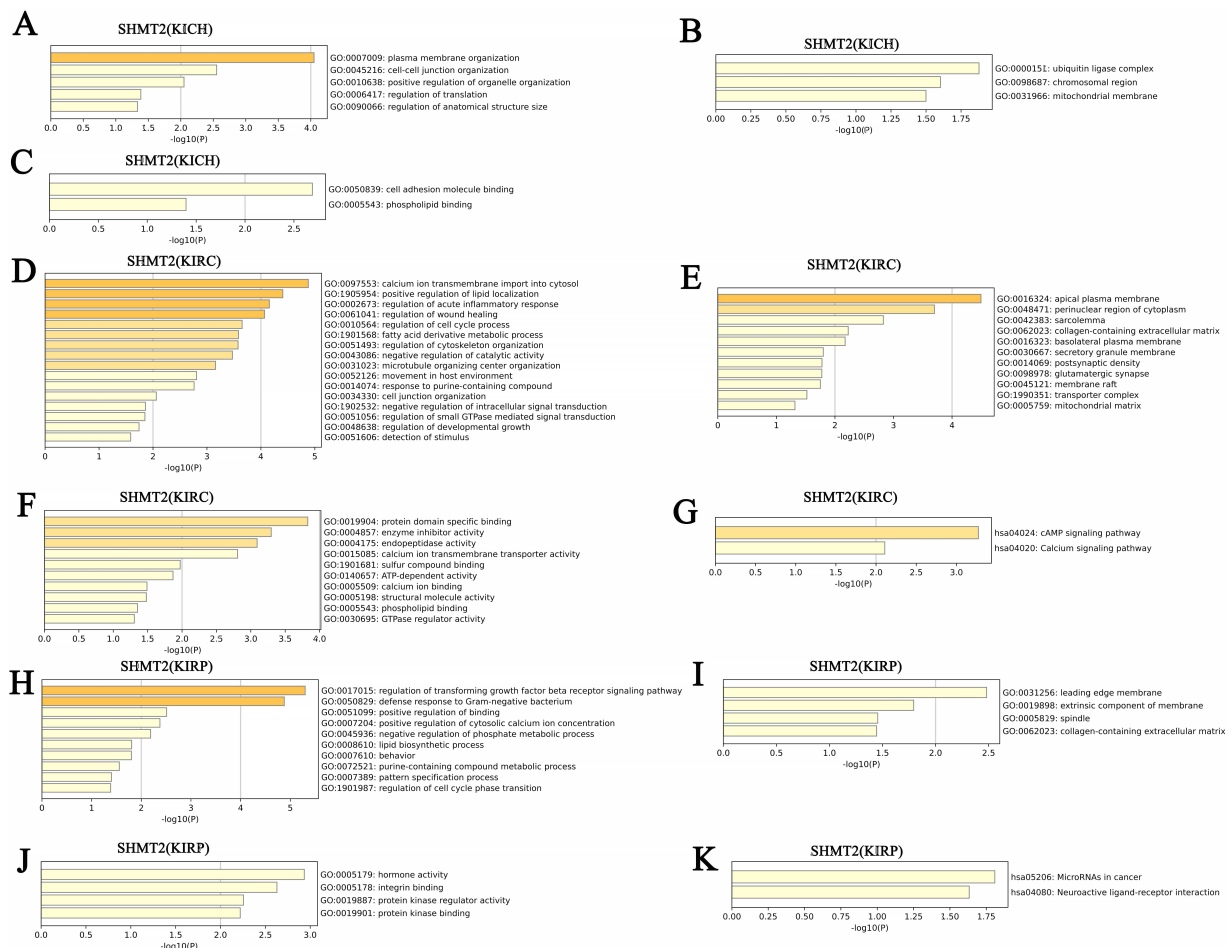


Fig. 11. GO function and KEGG pathways enrichment analyses of *SHMT2* and their NG in RCC (Metascape). (A) Biological processes of *SHMT2* and its NG in KICH. (B) Cellular components of *SHMT2* and its NG in KICH. (C) Molecular functions of *SHMT2* and its NG in KICH. (D) Biological processes of *SHMT2* and its NG in KIRC. (E) Cellular components of *SHMT2* and its NG in KIRC. (F) Molecular functions of *SHMT2* and its NG in KIRC. (G) KEGG pathway analysis of *SHMT2* and its NG in KIRC. (H) Biological processes of *SHMT2* and its NG in KIRP. (I) Cellular components of *SHMT2* and its NG in KIRP. (J) Molecular functions of *SHMT2* and its NG in KIRP. (K) KEGG pathway analysis of *SHMT2* and its NG in KIRP.

(Table 7). *PRODH* and *SHMT1* were the primary regulatory genes of *MYC*. In addition, *STAT1* was the critical transcription factor of *SHMT1* and its NG among patients with KIRC ($p < 0.05$) (Table 7). *STAT1* regulated the functions of *STAT2* and *TLR3*. Furthermore, *PPARG*, *NR3C1*, *HDAC1*, *STAT1*, and *MYC* were the critical transcription factors of *SHMT1* and its NG among patients with KIRP ($p < 0.05$) (Table 7). *SLC2A4*, *TP53*, and *TXNIP* were the primary regulatory genes of *PPARG*. *NR3C1* regulated the functions of *ATP1B1* and *TP53*. Moreover, *TP53* and *TXNIP* were the primary regulatory genes of *HDAC1*. *STAT1* regulated the functions of *FGFR3* and *TP53*. *SHMT1* and *TP53* were the central regulatory genes of *MYC*. However, we found that *AR* was the key transcription factor of *SHMT2* and its NG among patients with KICH ($p < 0.01$) (Table 8). *ATAD2* and *NDRG1* were the primary regulatory genes of *AR*. In addition, *SREBF2*, *MYCN*, and *SP3* were the key transcription factors of *SHMT2* and its NG

among patients with KIRC ($p < 0.05$) (Table 8). *SREBF2* regulated the functions of *ABCA1* and *LRP1*. *DDBI* and *EFNB3* were the central regulatory genes of *MYCN*. *SP3* regulated the functions of *ABCA1* and *ALOX12*. Furthermore, *FOXM1*, *DNMT1*, *REST*, and *E2F1* were the key transcription factors of *SHMT2* and its NG in KIRP ($p < 0.05$) (Table 8). *CDC25B* and *CDKN2A* were the central regulatory genes of *FOXM1*. *DNMT1* regulated the functions of *BMP2* and *CDKN2A*. Moreover, *AVP* and *CHGB* were the primary regulatory genes of *REST*. *E2F1* regulated the functions of *BMI1* and *CDKN2A*.

miRNA targets of *SHMT1* and *SHMT2* were analyzed using the LinkedOmics database. We found that (GCACTTT) miR-17-5P, miR-20A, miR-106A, miR-106B, miR-20B, and miR-519D; (TTTGCAC) miR-19A and miR-19B; and (AAGCCAT) miR-135A and miR-135B were the top three miRNA targets of *SHMT1* among patients with KICH ($p < 0.001$; Table 9). In addition,

Table 1. The top 50 SHMT1 NG alterations in KICH (cBioPortal).

Gene	Altered group	Unaltered group
<i>AP5Z1</i>	2 (33.33%)	0 (0.00%)
<i>BIRC3</i>	2 (33.33%)	0 (0.00%)
<i>DNAJC13</i>	2 (33.33%)	0 (0.00%)
<i>ENPP6</i>	2 (33.33%)	0 (0.00%)
<i>FAM47C</i>	2 (33.33%)	0 (0.00%)
<i>MTOR</i>	2 (33.33%)	0 (0.00%)
<i>MYO18B</i>	2 (33.33%)	0 (0.00%)
<i>OTOA</i>	2 (33.33%)	0 (0.00%)
<i>PACSI</i>	2 (33.33%)	0 (0.00%)
<i>PRODH</i>	2 (33.33%)	0 (0.00%)
<i>CNTN5</i>	2 (33.33%)	1 (1.67%)
<i>DMXL1</i>	2 (33.33%)	1 (1.67%)
<i>NLGN4X</i>	2 (33.33%)	1 (1.67%)
<i>SECISBP2L</i>	2 (33.33%)	1 (1.67%)
<i>ATRX</i>	2 (33.33%)	2 (3.33%)
<i>DNAH1</i>	2 (33.33%)	2 (3.33%)
<i>ZNF799</i>	2 (33.33%)	2 (3.33%)
<i>ABCC10</i>	1 (16.67%)	0 (0.00%)
<i>ABHD17A</i>	1 (16.67%)	0 (0.00%)
<i>ABTB2</i>	1 (16.67%)	0 (0.00%)
<i>ACPI</i>	1 (16.67%)	0 (0.00%)
<i>ACTBL2</i>	1 (16.67%)	0 (0.00%)
<i>ADAM17</i>	1 (16.67%)	0 (0.00%)
<i>ADAM19</i>	1 (16.67%)	0 (0.00%)
<i>ADAMTS16</i>	1 (16.67%)	0 (0.00%)
<i>ADGRB2</i>	1 (16.67%)	0 (0.00%)
<i>ADGRL1</i>	1 (16.67%)	0 (0.00%)
<i>ADH1C</i>	1 (16.67%)	0 (0.00%)
<i>ADII</i>	1 (16.67%)	0 (0.00%)
<i>ADORA2A</i>	1 (16.67%)	0 (0.00%)
<i>AGAP6</i>	1 (16.67%)	0 (0.00%)
<i>AGO3</i>	1 (16.67%)	0 (0.00%)
<i>AKAP9</i>	1 (16.67%)	0 (0.00%)
<i>ALKAL2</i>	1 (16.67%)	0 (0.00%)
<i>ALPK3</i>	1 (16.67%)	0 (0.00%)
<i>ALPL</i>	1 (16.67%)	0 (0.00%)
<i>ANKRD52</i>	1 (16.67%)	0 (0.00%)
<i>ANKRD66</i>	1 (16.67%)	0 (0.00%)
<i>AP1M1</i>	1 (16.67%)	0 (0.00%)
<i>AP1M2</i>	1 (16.67%)	0 (0.00%)
<i>AP2A1</i>	1 (16.67%)	0 (0.00%)
<i>AP3M2</i>	1 (16.67%)	0 (0.00%)
<i>APOBEC3G</i>	1 (16.67%)	0 (0.00%)
<i>ARHGEF39</i>	1 (16.67%)	0 (0.00%)
<i>ARHGEF40</i>	1 (16.67%)	0 (0.00%)
<i>ARRB1</i>	1 (16.67%)	0 (0.00%)
<i>ASAP2</i>	1 (16.67%)	0 (0.00%)
<i>ASIC4</i>	1 (16.67%)	0 (0.00%)
<i>ASPHD1</i>	1 (16.67%)	0 (0.00%)
<i>ATP11A</i>	1 (16.67%)	0 (0.00%)

Table 2. The top 50 SHMT1 NG alterations in KIRC (cBioPortal).

Gene	Altered group	Unaltered group
<i>MUC16</i>	9 (50.00%)	50 (11.68%)
<i>OVGP1</i>	7 (38.89%)	14 (3.27%)
<i>OR4N5</i>	6 (33.33%)	7 (1.64%)
<i>TLR3</i>	6 (33.33%)	8 (1.87%)
<i>BPIFC</i>	6 (33.33%)	9 (2.10%)
<i>BTRC</i>	6 (33.33%)	9 (2.10%)
<i>SLPI</i>	6 (33.33%)	11 (2.57%)
<i>TAS2R3</i>	6 (33.33%)	11 (2.57%)
<i>HEBP1</i>	6 (33.33%)	15 (3.50%)
<i>TSKS</i>	6 (33.33%)	15 (3.50%)
<i>CD4</i>	6 (33.33%)	16 (3.74%)
<i>MAP1B</i>	6 (33.33%)	16 (3.74%)
<i>PHACTR1</i>	6 (33.33%)	16 (3.74%)
<i>PDZD2</i>	6 (33.33%)	17 (3.97%)
<i>SSX3</i>	6 (33.33%)	17 (3.97%)
<i>ABCA6</i>	6 (33.33%)	18 (4.21%)
<i>TSHZ3</i>	6 (33.33%)	20 (4.67%)
<i>FAP</i>	5 (27.78%)	3 (0.70%)
<i>IL32</i>	5 (27.78%)	3 (0.70%)
<i>CCS</i>	5 (27.78%)	7 (1.64%)
<i>OSBPL3</i>	5 (27.78%)	7 (1.64%)
<i>NUMA1</i>	5 (27.78%)	8 (1.87%)
<i>OSBPL2</i>	5 (27.78%)	9 (2.10%)
<i>ZNF462</i>	5 (27.78%)	9 (2.10%)
<i>FYB1</i>	5 (27.78%)	10 (2.34%)
<i>LRP4</i>	5 (27.78%)	10 (2.34%)
<i>SLC8B1</i>	5 (27.78%)	10 (2.34%)
<i>C6</i>	5 (27.78%)	11 (2.57%)
<i>FAM104A</i>	5 (27.78%)	11 (2.57%)
<i>STAT2</i>	5 (27.78%)	12 (2.80%)
<i>NOMO1</i>	5 (27.78%)	13 (3.04%)
<i>NRSN2</i>	5 (27.78%)	13 (3.04%)
<i>CFAP53</i>	4 (22.22%)	3 (0.70%)
<i>EPG5</i>	4 (22.22%)	3 (0.70%)
<i>CWH43</i>	4 (22.22%)	4 (0.93%)
<i>FRYL</i>	4 (22.22%)	4 (0.93%)
<i>JAG1</i>	4 (22.22%)	4 (0.93%)
<i>ARFGEF2</i>	4 (22.22%)	5 (1.17%)
<i>KIF5A</i>	4 (22.22%)	5 (1.17%)
<i>PABIR3</i>	4 (22.22%)	5 (1.17%)
<i>SDHAF2</i>	4 (22.22%)	5 (1.17%)
<i>CCDC18</i>	4 (22.22%)	6 (1.40%)
<i>LGI2</i>	4 (22.22%)	6 (1.40%)
<i>NKDI</i>	4 (22.22%)	6 (1.40%)
<i>SLC12A9</i>	4 (22.22%)	6 (1.40%)
<i>MT-ND6</i>	3 (16.67%)	0 (0.00%)
<i>SLC4A11</i>	3 (16.67%)	0 (0.00%)
<i>STIM2</i>	3 (16.67%)	0 (0.00%)
<i>DIDO1</i>	3 (16.67%)	1 (0.23%)
<i>PDYN</i>	3 (16.67%)	1 (0.23%)

Table 3. The top 50 *SHMT1* NG alterations in KIRP (cBioPortal).

Gene	Altered group	Unaltered group
<i>STAG2</i>	4 (23.53%)	4 (1.52%)
<i>FH</i>	3 (17.65%)	1 (0.38%)
<i>FGFR3</i>	3 (17.65%)	2 (0.76%)
<i>CRISP3</i>	2 (11.76%)	0 (0.00%)
<i>LLGL1</i>	2 (11.76%)	0 (0.00%)
<i>MINK1</i>	2 (11.76%)	0 (0.00%)
<i>SAYS1</i>	2 (11.76%)	0 (0.00%)
<i>SNRPE</i>	2 (11.76%)	0 (0.00%)
<i>TRPV2</i>	2 (11.76%)	0 (0.00%)
<i>TP53</i>	3 (17.65%)	5 (1.90%)
<i>CACNG2</i>	2 (11.76%)	1 (0.38%)
<i>CCNL2</i>	2 (11.76%)	1 (0.38%)
<i>DNAJA2</i>	2 (11.76%)	1 (0.38%)
<i>ITGAE</i>	2 (11.76%)	1 (0.38%)
<i>ITGAL</i>	2 (11.76%)	1 (0.38%)
<i>KIAA0753</i>	2 (11.76%)	1 (0.38%)
<i>NDC80</i>	2 (11.76%)	1 (0.38%)
<i>NUP88</i>	2 (11.76%)	1 (0.38%)
<i>PABPN1</i>	2 (11.76%)	1 (0.38%)
<i>SLC29A1</i>	2 (11.76%)	1 (0.38%)
<i>SLC2A4</i>	2 (11.76%)	1 (0.38%)
<i>TMEM212</i>	2 (11.76%)	1 (0.38%)
<i>TXNIP</i>	2 (11.76%)	1 (0.38%)
<i>WDR59</i>	2 (11.76%)	1 (0.38%)
<i>ZNF689</i>	2 (11.76%)	1 (0.38%)
<i>ATP1B1</i>	3 (17.65%)	6 (2.28%)
<i>ALYREF</i>	2 (11.76%)	2 (0.76%)
<i>ANAPC11</i>	2 (11.76%)	2 (0.76%)
<i>ARHGDI1</i>	2 (11.76%)	2 (0.76%)
<i>ARL16</i>	2 (11.76%)	2 (0.76%)
<i>CCDC137</i>	2 (11.76%)	2 (0.76%)
<i>DEFB110</i>	2 (11.76%)	2 (0.76%)
<i>GCGR</i>	2 (11.76%)	2 (0.76%)
<i>HSDL2</i>	2 (11.76%)	2 (0.76%)
<i>IFNA10</i>	2 (11.76%)	2 (0.76%)
<i>IFNA14</i>	2 (11.76%)	2 (0.76%)
<i>IFNA16</i>	2 (11.76%)	2 (0.76%)
<i>IFNA17</i>	2 (11.76%)	2 (0.76%)
<i>IFNA21</i>	2 (11.76%)	2 (0.76%)
<i>IFNA4</i>	2 (11.76%)	2 (0.76%)
<i>IFNA7</i>	2 (11.76%)	2 (0.76%)
<i>IFNW1</i>	2 (11.76%)	2 (0.76%)
<i>KIF19</i>	2 (11.76%)	2 (0.76%)
<i>MAFG</i>	2 (11.76%)	2 (0.76%)
<i>MCRIP1</i>	2 (11.76%)	2 (0.76%)
<i>MEP1A</i>	2 (11.76%)	2 (0.76%)
<i>MRPL12</i>	2 (11.76%)	2 (0.76%)
<i>MYADML2</i>	2 (11.76%)	2 (0.76%)
<i>NPB</i>	2 (11.76%)	2 (0.76%)
<i>P4HB</i>	2 (11.76%)	2 (0.76%)

Table 4. The top 50 *SHMT2* NG alterations in KICH (cBioPortal).

Gene	Altered group	Unaltered group
<i>AARD</i>	2 (100.00%)	0 (0.00%)
<i>ASAP1</i>	2 (100.00%)	0 (0.00%)
<i>ATAD2</i>	2 (100.00%)	0 (0.00%)
<i>C8ORF76</i>	2 (100.00%)	0 (0.00%)
<i>CASC8</i>	2 (100.00%)	0 (0.00%)
<i>CCAT1</i>	2 (100.00%)	0 (0.00%)
<i>CCDC26</i>	2 (100.00%)	0 (0.00%)
<i>CCN3</i>	2 (100.00%)	0 (0.00%)
<i>CCN4</i>	2 (100.00%)	0 (0.00%)
<i>COLEC10</i>	2 (100.00%)	0 (0.00%)
<i>CYRIB</i>	2 (100.00%)	0 (0.00%)
<i>DEPTOR</i>	2 (100.00%)	0 (0.00%)
<i>DERL1</i>	2 (100.00%)	0 (0.00%)
<i>DSCC1</i>	2 (100.00%)	0 (0.00%)
<i>EFR3A</i>	2 (100.00%)	0 (0.00%)
<i>EIF3H</i>	2 (100.00%)	0 (0.00%)
<i>EXT1</i>	2 (100.00%)	0 (0.00%)
<i>FAM83A</i>	2 (100.00%)	0 (0.00%)
<i>FAM91A1</i>	2 (100.00%)	0 (0.00%)
<i>FBXO32</i>	2 (100.00%)	0 (0.00%)
<i>FER1L6</i>	2 (100.00%)	0 (0.00%)
<i>GSDMC</i>	2 (100.00%)	0 (0.00%)
<i>HHLA1</i>	2 (100.00%)	0 (0.00%)
<i>HPYR1</i>	2 (100.00%)	0 (0.00%)
<i>KCNQ3</i>	2 (100.00%)	0 (0.00%)
<i>KHDRBS3</i>	2 (100.00%)	0 (0.00%)
<i>KLHL38</i>	2 (100.00%)	0 (0.00%)
<i>LINC00861</i>	2 (100.00%)	0 (0.00%)
<i>LINC00964</i>	2 (100.00%)	0 (0.00%)
<i>LINC00977</i>	2 (100.00%)	0 (0.00%)
<i>LINC02912</i>	2 (100.00%)	0 (0.00%)
<i>LRATD2</i>	2 (100.00%)	0 (0.00%)
<i>MED30</i>	2 (100.00%)	0 (0.00%)
<i>MRPL13</i>	2 (100.00%)	0 (0.00%)
<i>MTSS1</i>	2 (100.00%)	0 (0.00%)
<i>NDRG1</i>	2 (100.00%)	0 (0.00%)
<i>NDUFB9</i>	2 (100.00%)	0 (0.00%)
<i>NSMCE2</i>	2 (100.00%)	0 (0.00%)
<i>NTAQ1</i>	2 (100.00%)	0 (0.00%)
<i>OC90</i>	2 (100.00%)	0 (0.00%)
<i>PCAT1</i>	2 (100.00%)	0 (0.00%)
<i>PCAT2</i>	2 (100.00%)	0 (0.00%)
<i>PLEC</i>	2 (100.00%)	0 (0.00%)
<i>POU5F1B</i>	2 (100.00%)	0 (0.00%)
<i>PVT1</i>	2 (100.00%)	0 (0.00%)
<i>RAD21</i>	2 (100.00%)	0 (0.00%)
<i>RN7SKP153</i>	2 (100.00%)	0 (0.00%)
<i>RN7SKP155</i>	2 (100.00%)	0 (0.00%)
<i>RN7SKP206</i>	2 (100.00%)	0 (0.00%)
<i>RN7SKP226</i>	2 (100.00%)	0 (0.00%)

Table 5. The top 50 *SHMT2* NG alterations in KIRC (cBioPortal).

Gene	Altered group	Unaltered group
<i>PAPPA2</i>	6 (31.58%)	17 (3.98%)
<i>C3</i>	6 (31.58%)	15 (3.51%)
<i>PREP</i>	5 (26.32%)	6 (1.41%)
<i>EFNB3</i>	5 (26.32%)	7 (1.64%)
<i>CST4</i>	5 (26.32%)	8 (1.87%)
<i>ALOX12</i>	5 (26.32%)	11 (2.58%)
<i>GLII</i>	5 (26.32%)	12 (2.81%)
<i>KLK1</i>	5 (26.32%)	12 (2.81%)
<i>MRPL24</i>	5 (26.32%)	13 (3.04%)
<i>KIAA0408</i>	5 (26.32%)	14 (3.28%)
<i>ATP2B4</i>	5 (26.32%)	15 (3.51%)
<i>CACNA1S</i>	5 (26.32%)	16 (3.75%)
<i>DDB1</i>	5 (26.32%)	16 (3.75%)
<i>HEBP1</i>	5 (26.32%)	16 (3.75%)
<i>LRP1</i>	5 (26.32%)	16 (3.75%)
<i>ABCA1</i>	5 (26.32%)	17 (3.98%)
<i>ARFGEF1</i>	5 (26.32%)	17 (3.98%)
<i>CD4</i>	5 (26.32%)	17 (3.98%)
<i>MAP1B</i>	5 (26.32%)	17 (3.98%)
<i>MUC17</i>	5 (26.32%)	17 (3.98%)
<i>CNTROB</i>	4 (21.05%)	2 (0.47%)
<i>NETO2</i>	4 (21.05%)	3 (0.70%)
<i>OR10G2</i>	4 (21.05%)	3 (0.70%)
<i>SENP6</i>	4 (21.05%)	4 (0.94%)
<i>ARHGEF40</i>	4 (21.05%)	5 (1.17%)
<i>ATNI</i>	4 (21.05%)	5 (1.17%)
<i>PPP1R10</i>	4 (21.05%)	5 (1.17%)
<i>TMCC3</i>	4 (21.05%)	5 (1.17%)
<i>OR52B6</i>	4 (21.05%)	7 (1.64%)
<i>DGKA</i>	4 (21.05%)	8 (1.87%)
<i>PKD2</i>	4 (21.05%)	8 (1.87%)
<i>ACSM2A</i>	4 (21.05%)	9 (2.11%)
<i>ADAMTS8</i>	4 (21.05%)	9 (2.11%)
<i>ASHIL</i>	4 (21.05%)	9 (2.11%)
<i>DUOX1</i>	4 (21.05%)	9 (2.11%)
<i>HMGCLL1</i>	3 (15.79%)	0 (0.00%)
<i>ATRN</i>	3 (15.79%)	1 (0.23%)
<i>C9ORF152</i>	3 (15.79%)	1 (0.23%)
<i>TMEM30A</i>	3 (15.79%)	1 (0.23%)
<i>WDR27</i>	3 (15.79%)	1 (0.23%)
<i>CCN2</i>	3 (15.79%)	2 (0.47%)
<i>CD109</i>	3 (15.79%)	2 (0.47%)
<i>FILIP1</i>	3 (15.79%)	2 (0.47%)
<i>MFSD4B</i>	3 (15.79%)	2 (0.47%)
<i>PATJ</i>	3 (15.79%)	2 (0.47%)
<i>PTGER3</i>	3 (15.79%)	2 (0.47%)
<i>SLITRK2</i>	3 (15.79%)	2 (0.47%)
<i>ERN2</i>	3 (15.79%)	3 (0.70%)
<i>SIRPA</i>	3 (15.79%)	3 (0.70%)
<i>TROAP</i>	3 (15.79%)	3 (0.70%)

Table 6. The top 50 *SHMT2* NG alterations in KIRP (cBioPortal).

Gene	Altered group	Unaltered group
<i>CDKN2A</i>	5 (25.00%)	10 (3.85%)
<i>SIRPA</i>	3 (15.00%)	0 (0.00%)
<i>ARHGAP21</i>	3 (15.00%)	1 (0.38%)
<i>PAK5</i>	3 (15.00%)	1 (0.38%)
<i>CPXMI</i>	3 (15.00%)	2 (0.77%)
<i>GRAMD1A</i>	3 (15.00%)	2 (0.77%)
<i>SRD5A1</i>	3 (15.00%)	2 (0.77%)
<i>ADAM33</i>	2 (10.00%)	0 (0.00%)
<i>ADRA1D</i>	2 (10.00%)	0 (0.00%)
<i>ANGPT4</i>	2 (10.00%)	0 (0.00%)
<i>AP5S1</i>	2 (10.00%)	0 (0.00%)
<i>ATRN</i>	2 (10.00%)	0 (0.00%)
<i>ATXN3L</i>	2 (10.00%)	0 (0.00%)
<i>AVP</i>	2 (10.00%)	0 (0.00%)
<i>BMI1</i>	2 (10.00%)	0 (0.00%)
<i>BMP2</i>	2 (10.00%)	0 (0.00%)
<i>C20ORF141</i>	2 (10.00%)	0 (0.00%)
<i>C20ORF202</i>	2 (10.00%)	0 (0.00%)
<i>C20ORF27</i>	2 (10.00%)	0 (0.00%)
<i>C20ORF96</i>	2 (10.00%)	0 (0.00%)
<i>CDC25B</i>	2 (10.00%)	0 (0.00%)
<i>CDS2</i>	2 (10.00%)	0 (0.00%)
<i>CHGB</i>	2 (10.00%)	0 (0.00%)
<i>COL20A1</i>	2 (10.00%)	0 (0.00%)
<i>CRLS1</i>	2 (10.00%)	0 (0.00%)
<i>DDRGK1</i>	2 (10.00%)	0 (0.00%)
<i>DEFB125</i>	2 (10.00%)	0 (0.00%)
<i>DEFB126</i>	2 (10.00%)	0 (0.00%)
<i>DEFB127</i>	2 (10.00%)	0 (0.00%)
<i>DEFB128</i>	2 (10.00%)	0 (0.00%)
<i>DEFB129</i>	2 (10.00%)	0 (0.00%)
<i>DEFB132</i>	2 (10.00%)	0 (0.00%)
<i>EBF4</i>	2 (10.00%)	0 (0.00%)
<i>ENKUR</i>	2 (10.00%)	0 (0.00%)
<i>FAM110A</i>	2 (10.00%)	0 (0.00%)
<i>FAM47B</i>	2 (10.00%)	0 (0.00%)
<i>FASTKD5</i>	2 (10.00%)	0 (0.00%)
<i>FERMT1</i>	2 (10.00%)	0 (0.00%)
<i>FKBP1A</i>	2 (10.00%)	0 (0.00%)
<i>FRMD5</i>	2 (10.00%)	0 (0.00%)
<i>GFRA4</i>	2 (10.00%)	0 (0.00%)
<i>GNRH2</i>	2 (10.00%)	0 (0.00%)
<i>GPRI74</i>	2 (10.00%)	0 (0.00%)
<i>GRIPAP1</i>	2 (10.00%)	0 (0.00%)
<i>HACD1</i>	2 (10.00%)	0 (0.00%)
<i>HAUS6</i>	2 (10.00%)	0 (0.00%)
<i>HSPA12B</i>	2 (10.00%)	0 (0.00%)
<i>ITGA8</i>	2 (10.00%)	0 (0.00%)
<i>ITPA</i>	2 (10.00%)	0 (0.00%)
<i>LAMP5</i>	2 (10.00%)	0 (0.00%)

Table 7. Key regulated factor of *SHMT1* and the top 50 NG in renal cell carcinoma (TRRUST).

Type	Key TF	Description	Regulated gene	<i>p</i> -value
KICH	MYC	v-myc myelocytomatosis viral oncogene homolog (avian)	<i>PRODH, SHMT1</i>	0.03
KIRC	STAT1	signal transducer and activator of transcription 1	<i>STAT2, TLR3</i>	0.0193
KIRP	PPARG	peroxisome proliferator-activated receptor gamma	<i>SLC2A4, TP53, TXNIP</i>	0.000755
	NR3C1	nuclear receptor subfamily 3, group C, member 1	<i>ATP1B1, TP53</i>	0.00473
	HDAC1	histone deacetylase 1	<i>TP53, TXNIP</i>	0.0158
	STAT1	signal transducer and activator of transcription 1	<i>FGFR3, TP53</i>	0.0217
	MYC	v-myc myelocytomatosis viral oncogene homolog (avian)	<i>SHMT1, TP53</i>	0.03

Table 8. Key regulated factor of *SHMT2* and the top 50 NG in renal cell carcinoma (TRRUST).

Type	Key TF	Description	Regulated gene	<i>p</i> -value
KICH	AR	androgen receptor	<i>ATAD2, NDRG1</i>	0.00895
KIRC	SREBF2	sterol regulatory element binding transcription factor 2	<i>ABCA1, LRPI</i>	0.00122
	MYCN	v-myc myelocytomatosis viral related oncogene, neuroblastoma derived (avian)	<i>DDBI, EFNB3</i>	0.00609
	SP3	Sp3 transcription factor	<i>ABCA1, ALOX12</i>	0.0348
KIRP	FOXM1	forkhead box M1	<i>CDC25B, CDKN2A</i>	0.000806
	DNMT1	DNA (cytosine-5-)-methyltransferase 1	<i>BMP2, CDKN2A</i>	0.0027
	REST	RE1-silencing transcription factor	<i>AVP, CHGB</i>	0.00287
	E2F1	E2F transcription factor 1	<i>BMI1, CDKN2A</i>	0.044

tion, the top three miRNA targets of *SHMT1* among patients with KIRC were (AAGTCCA) miR-422B and miR-422A, (GCTTGAA) miR-498, and (GGGGCCC) miR-296 ($p < 0.001$; Table 9). Furthermore, (CAGGTCC) miR-492, (ACTGAAA) miR-30A-3P and miR-30E-3P, and (CTTTGTA) miR-524 were the top three miRNA targets of *SHMT1* in KIRP ($p < 0.001$; Table 9). However, (AAGCAAT) miR-137, (GGGCATT) miR-365, and (AACATTC) miR-409-3P were the top three miRNA targets of *SHMT2* in KICH ($p < 0.001$; Table 10). The top three miRNA targets of *SHMT2* in KIRC were (ACTGAAA) miR-30A-3P and miR-30E-3P, (CATGTAA) miR-496, and (AGCATTA) miR-155 ($p < 0.001$; Table 10). Moreover, (ATGTACA) miR-493, (GGGCATT) miR-365, and (CTTTGCA) miR-527 were the top three miRNA targets of *SHMT2* in KIRP ($p < 0.001$; Table 10).

3.6 Correlation of Differentially Expressed Genes and *SHMT* Expression in RCC

The mRNA sequencing data from patients with KICH (n = 66), KIRC (n = 533), and KIRP (n = 290), using the LinkedOmics database, were analyzed. Results indicated that the expression of 19,216 genes was correlated with *SHMT1* expression in KICH. The 10,757 and 8459 genes were positively and negatively correlated with *SHMT1* expression, respectively (Fig. 12A). We screened 50 genes whose expression levels were significantly correlated with *SHMT1* expression in KICH ($p < 0.05$; Fig. 12B,C). *PRODH* (Pearson correlation coefficient (PCO) = 0.7353, $p = 2.05 \times 10^{-12}$; Fig. 13A), *SH3KBPI* (PCO = 0.7242, $p = 6.321 \times 10^{-12}$; Fig. 13B), and *EML6* (PCO = 0.7169, $p = 1.288 \times 10^{-11}$; Fig. 13C) were the top three genes whose expression levels were positively correlated with

SHMT1 expression. In addition, the expression levels of 20,158 genes were correlated with *SHMT1* expression in KIRC. A total of 9036 and 11,122 genes were positively and negatively correlated with *SHMT1* expression, respectively (Fig. 12D). We screened 50 genes whose expression levels were significantly correlated with *SHMT1* expression in KIRC ($p < 0.05$; Fig. 12E,F). Among the screened genes, *ACSM2B* (PCO = 0.7968, $p = 2.754 \times 10^{-118}$; Fig. 13D), *ACSM2A* (PCO = 0.792, $p = 7.393 \times 10^{-116}$; Fig. 13E), and *PDZK1* (PCO = 0.7817, $p = 5.842 \times 10^{-111}$; Fig. 13F) were the top three genes whose expression levels were positively correlated with *SHMT1* expression. Furthermore, the expression levels of 20,023 genes were correlated with *SHMT1* expression in KIRP, of which 8091 and 11,932 genes were positively and negatively correlated with *SHMT1* expression, respectively (Fig. 12G). In addition, we screened 50 genes whose expression levels were significantly positively and negatively correlated with *SHMT1* expression in KIRP ($p < 0.05$; Fig. 12H,I). Among the screened genes, *SMTNL2* (PCO = 0.8186, $p = 2.592 \times 10^{-71}$; Fig. 13G), *ACSM2A* (PCO = 0.7928, $p = 6.781 \times 10^{-64}$; Fig. 13H), and *ACSM5* (PCO = 0.7911, $p = 1.956 \times 10^{-63}$; Fig. 13I) were the top three genes whose expression levels were positively correlated with *SHMT1* expression.

Our results showed that the expression levels of 19,216 genes were correlated with *SHMT2* expression in KICH. Moreover, 10,436 and 8780 genes were positively and negatively correlated with *SHMT2* expression, respectively (Fig. 14A). We screened 50 genes whose expression levels were significantly positively and negatively correlated with *SHMT2* expression in KICH ($p < 0.05$; Fig. 14B,C). *PSATI* (PCO = 0.7665, $p = 6.356 \times 10^{-14}$; Fig. 15A), *ASNS* (PCO = 0.7594, $p = 1.458 \times 10^{-13}$;

Table 9. The top three miRNA targets of *SHMT1* in renal cell carcinoma (LinkedOmics).

Type	Enriched category	Gene set	Leading edge number	<i>p</i> -value
KICH	miRNA Target	GCACTTT, miR-17-5P, miR-20A, miR-106A, miR-106B, miR-20B, miR-519D	111	0.001
		TTTGAC, miR-19A, miR-19B	96	0.001
		AAGCCAT, miR-135A, miR-135B	58	0.001
KIRC	miRNA Target	AAGTCCA, miR-422B, miR-422A	23	0.001
		GCTTGAA, miR-498	26	0.001
		GGGGCCC, miR-296	11	0.001
KIRP	miRNA Target	CAGGTCC, miR-492	22	0.001
		ACTGAAA, miR-30A-3P, miR-30E-3P	68	0.001
		CTTTGTA, miR-524	137	0.001

Table 10. The top three miRNA targets of *SHMT2* in renal cell carcinoma (LinkedOmics).

Type	Enriched category	Gene set	Leading edge number	<i>p</i> -value
KICH	miRNA Target	AAGCAAT, miR-137	48	0.001
		GGGCATT, miR-365	22	0.001
		AACATTC, miR-409-3P	31	0.001
KIRC	miRNA Target	ACTGAAA, miR-30A-3P, miR-30E-3P	72	0.001
		CATGTAA, miR-496	62	0.001
		AGCATTA, miR-155	48	0.001
KIRP	miRNA Target	ATGTACA, miR-493	101	0.001
		GGGCATT, miR-365	46	0.001
		CTTTGCA, miR-527	66	0.001

Fig. 15B), and *YARS* (PCO = 0.7573, $p = 1.871 \times 10^{-13}$; Fig. 15C) were the top three genes whose expression levels were positively correlated with *SHMT2* expression. However, the expression levels of 20,158 genes were correlated with *SHMT2* expression among patients with KIRC; of which 10,443 and 9715 genes were positively and negatively correlated with *SHMT2* expression, respectively (Fig. 14D). Additionally, we screened 50 genes whose expression levels were significantly positively and negatively correlated with *SHMT2* expression among patients with KIRC ($p < 0.05$; Fig. 14E,F). *NDUFA4L2* (PCO = 0.6471, $p = 1.481 \times 10^{-64}$; Fig. 15D), *RALGPS1* (PCO = -0.5957, $p = 1.684 \times 10^{-52}$; Fig. 15E), and *NOL3* (PCO = 0.5789, $p = 5.235 \times 10^{-49}$; Fig. 15F) were the top three genes whose expression levels were positively or negatively correlated with *SHMT2* expression. Furthermore, the expression levels of 20,023 genes were correlated with *SHMT2* expression among patients with KIRP; of which 9759 and 10,264 genes were positively and negatively correlated with *SHMT2* expression, respectively (Fig. 14G). We also screened 50 genes whose expression levels were significantly positively and negatively correlated with *SHMT2* expression among patients with KIRP ($p < 0.05$; Fig. 14H,I). *CDK4* (PCO = 0.6734, $p = 1.154 \times 10^{-39}$; Fig. 15G), *GK5* (PCO = -0.6554, $p = 5.696 \times 10^{-37}$; Fig. 15H), and *C12orf52* (PCO = 0.6466, $p = 9.859 \times 10^{-36}$; Fig. 15I) were the top three genes whose expression levels were positively or negatively correlated with *SHMT2* expression.

3.7 Immune Cell Infiltration and *SHMT* Expression in RCC

The TIMER database was used to evaluate the relationship of immune cell infiltration levels with *SHMT1* and *SHMT2* expression among patients with RCC. Results showed that *SHMT1* expression was positively correlated with B-cell (Cor = 0.308, $p = 1.25 \times 10^{-2}$) and dendritic cell infiltration levels (Cor = 0.421, $p = 4.82 \times 10^{-4}$; Fig. 16A) in KICH. The *SHMT1* expression was positively correlated with B-cell infiltration level in KIRC (Cor = 0.161, $p = 5.42 \times 10^{-4}$; Fig. 16B). In addition, *SHMT1* expression was positively correlated with macrophage infiltration levels in KIRP (Cor = 0.257, $p = 3.97 \times 10^{-5}$; Fig. 16C). However, B-cell (Cor = -0.227, $p = 2.56 \times 10^{-4}$; Fig. 16C) and CD8+ T-cell (Cor = -0.226, $p = 2.58 \times 10^{-4}$; Fig. 16C) infiltration levels were negatively correlated with *SHMT1* expression in KIRP. The *SHMT2* expression was positively correlated with CD4+ T-cell (Cor = 0.363, $p = 2.98 \times 10^{-3}$), neutrophil (Cor = 0.397, $p = 1.07 \times 10^{-3}$), and dendritic cell (Cor = 0.312, $p = 1.14 \times 10^{-2}$) infiltration levels in KICH (Fig. 16D). *SHMT2* expression was positively correlated with B-cell (Cor = 0.229, $p = 2.19 \times 10^{-4}$; Fig. 16F) and CD8+ T-cell (Cor = 0.319, $p = 1.69 \times 10^{-7}$) infiltration levels in KIRP (Fig. 16F).

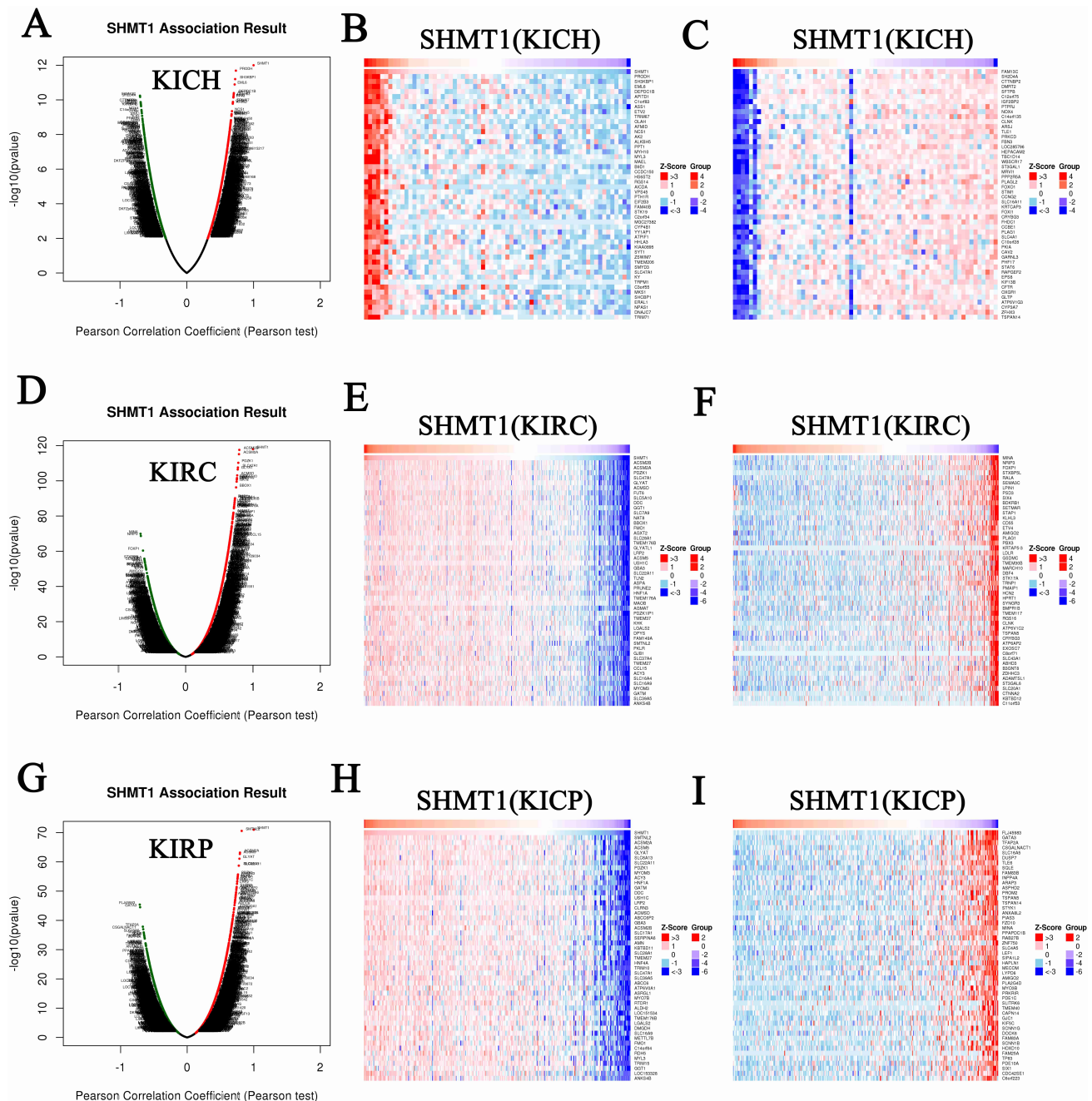


Fig. 12. Genes differentially expressed in correlation with *SHMT1* expression in RCC (LinkedOmics). (A) A Pearson test was used to analyze correlations between *SHMT1* expression and genes differentially expressed in patients with KICH. (B,C) Heatmaps showing positively and negatively expressed genes correlated with *SHMT1* expression in patients with KICH. (D) A Pearson test was used to analyze correlations between *SHMT1* expression and genes differentially expressed in patients with KIRC. (E,F) Heatmaps showing genes whose expression positively and negatively correlated with *SHMT1* expression in patients with KIRC. (G) A Pearson test was used to analyze correlations between *SHMT1* expression and genes differentially expressed in patients with KIRP. (H,I) Heatmaps showing genes whose expression positively and negatively correlated with *SHMT1* expression in patients with KIRP.

4. Discussion

Metabolic reprogramming is an essential hallmark of cancer development. Normal cells typically rely on the uptake of serine/glycine from the environment. However, some cancer subtypes synthesize their own serine/glycine intracellularly and become dependent to synthesis [21,22]

by relying on intracellular serine synthesis to meet the high demands of cancer cells, synthesize purines, control redox homeostasis, regulate DNA methylation, and support lipid metabolism [22]. As a result, tumor growth, differentiation, and metastasis are promoted. *SHMT* is a central enzyme for metabolic reprogramming in cancer cells,

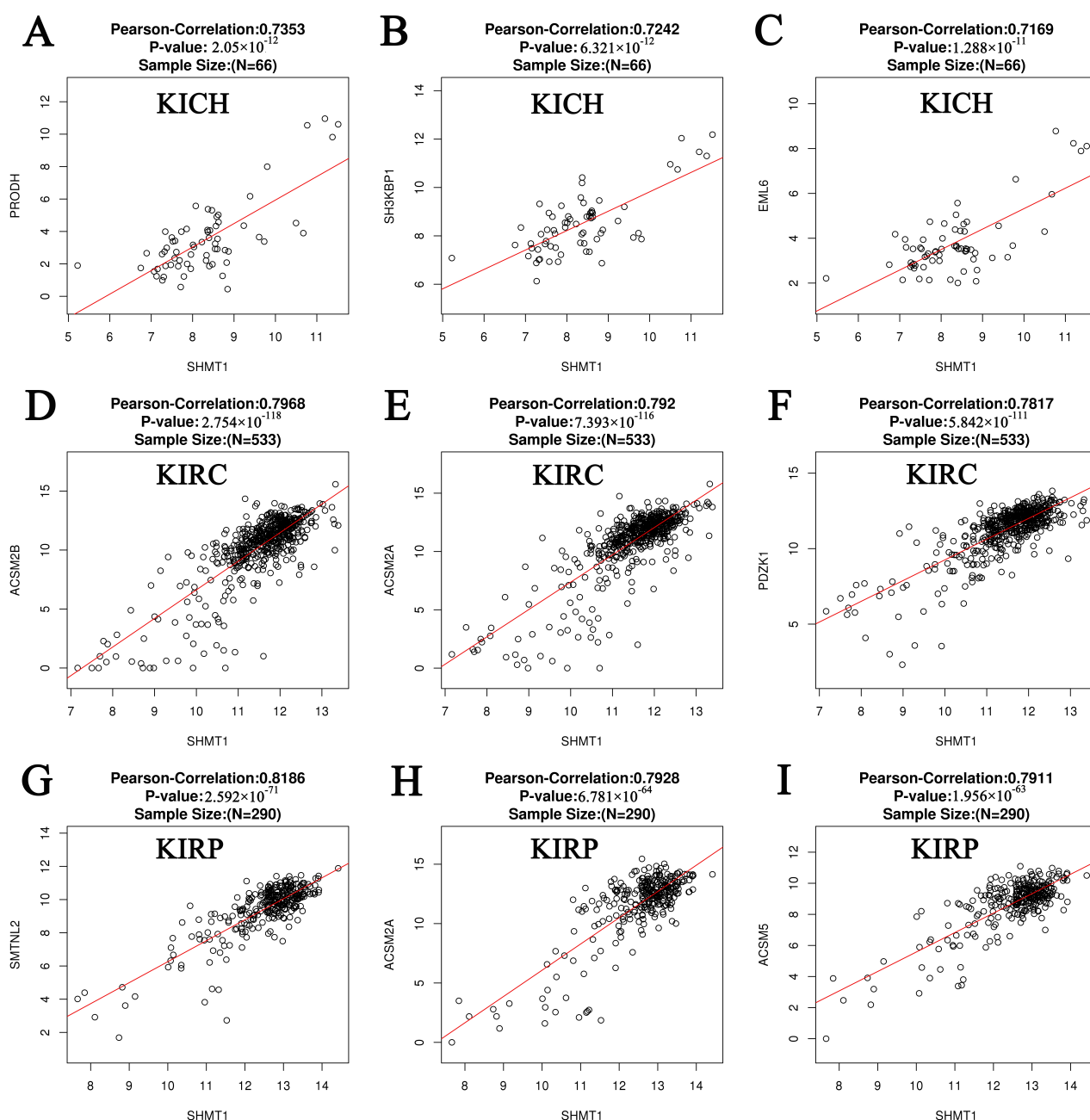


Fig. 13. Pearson correlation analysis of gene expression and *SHMT1* in RCC (LinkedOmics). (A) *PRODH* in patients with KICH. (B) *SH3KBP1* in patients with KICH. (C) *EML6* in patients with KICH. (D) *ACSM2B* in patients with KIRC. (E) *ACSM2A* in patients with KIRC. (F) *PDZK1* in patients with KIRC. (G) *SMTNL2* in patients with KIRP. (H) *ACSM2A* in patients with KIRP. (I) *ACSM5* in patients with KIRP.

which activates a carbon unit in serine-glycine one-carbon metabolism. Previous studies have shown that *SHMT1* and *SHMT2* are highly upregulated in some cancers [23]. However, the expression, prognosis, gene regulation network, and regulatory targets of *SHMT1* and *SHMT2* have not been reported in patients with RCC.

The expression levels of *SHMT1* and *SHMT2* were compared in patients with RCC based on sample type, individual cancer stage, sex, and patient age. This study

found that *SHMT2* transcript levels were significantly upregulated in patients with KICH, KIRC, and KIRP. Contrary to previous findings [23], *SHMT1* expression was significantly downregulated in these patients. Our results showed that *SHMT1* transcript levels in patients with KIRC were significantly upregulated in females compared to that in males. However, *SHMT1* transcript levels were significantly downregulated and *SHMT2* transcript levels were upregulated in female patients with KIRP compared to those

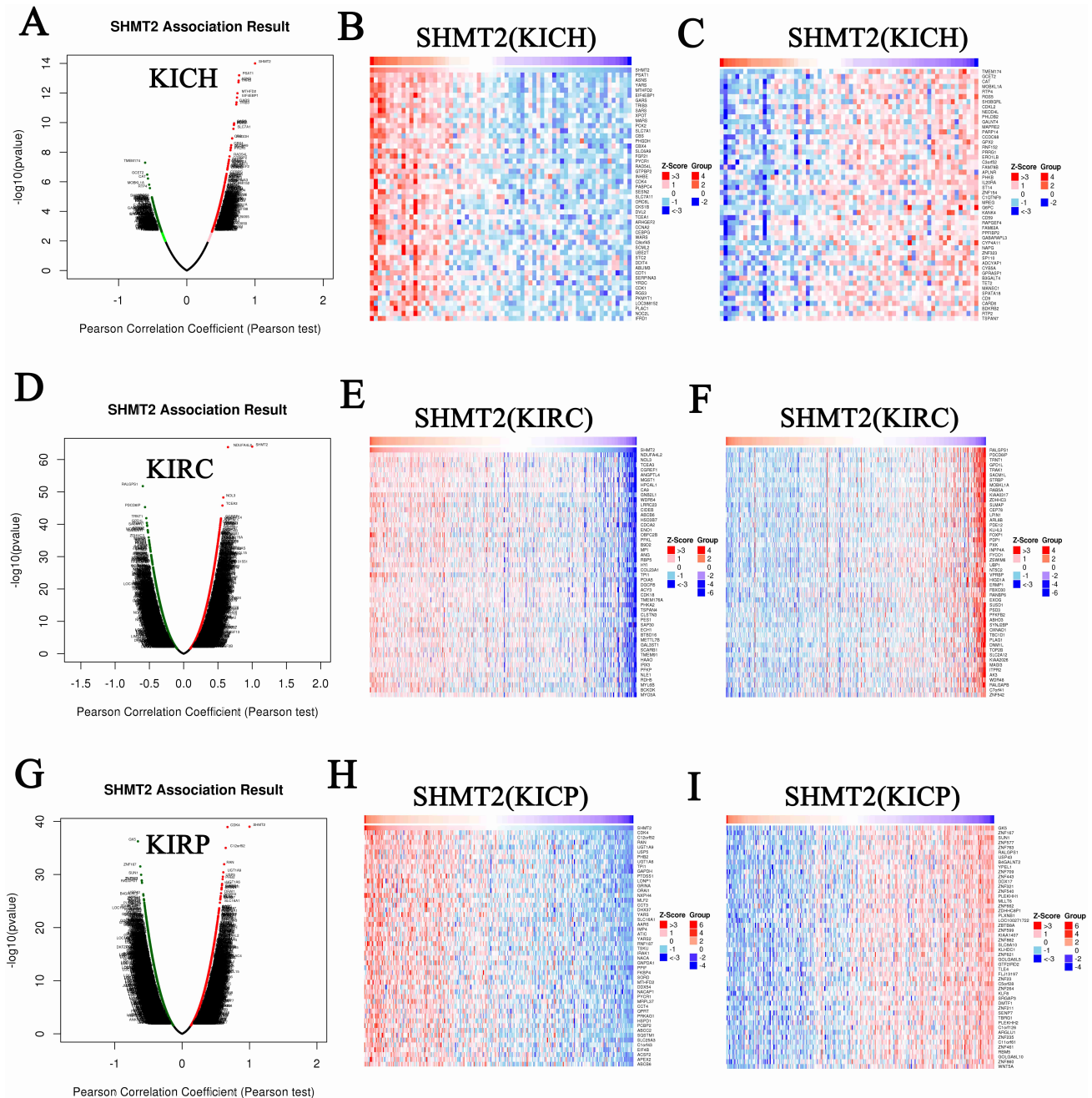


Fig. 14. Genes differentially expressed in correlation with *SHMT2* expression in RCC (LinkedOmics). (A) A Pearson test was used to analyze correlations between *SHMT2* expression and genes differentially expressed in patients with KICH. (B,C) Heat maps showing genes whose expression positively and negatively correlated with *SHMT2* expression in patients with KICH. (D) A Pearson test was used to analyze correlations between *SHMT2* expression and genes differentially expressed in patients with KIRC. (E,F) Heat maps showing genes whose expression positively and negatively correlated with *SHMT2* expression in patients with KIRC. (G) A Pearson test was used to analyze correlations between *SHMT2* expression and genes differentially expressed in patients with KIRP. (H,I) Heat maps showing genes whose expression positively and negatively correlated with *SHMT2* expression in patients with KIRP.

in the corresponding male patients. Nevertheless, this finding has not been previously reported. The differential expression of *SHMT1* and *SHMT2* between the sexes merits increased attention. This may be an essential basis for the differential treatment of *SHMT* targets in male and female patients with RCC.

Furthermore, a significant positive correlation between *SHMT1* expression and the pathological stages of KIRC and KIRP was found. Similarly, there was a significant positive correlation between *SHMT2* expression and the pathological stages of KICH and KIRP. *SHMT1* versus *SHMT2* were altered by 9% vs 3% (n = 66 patients with

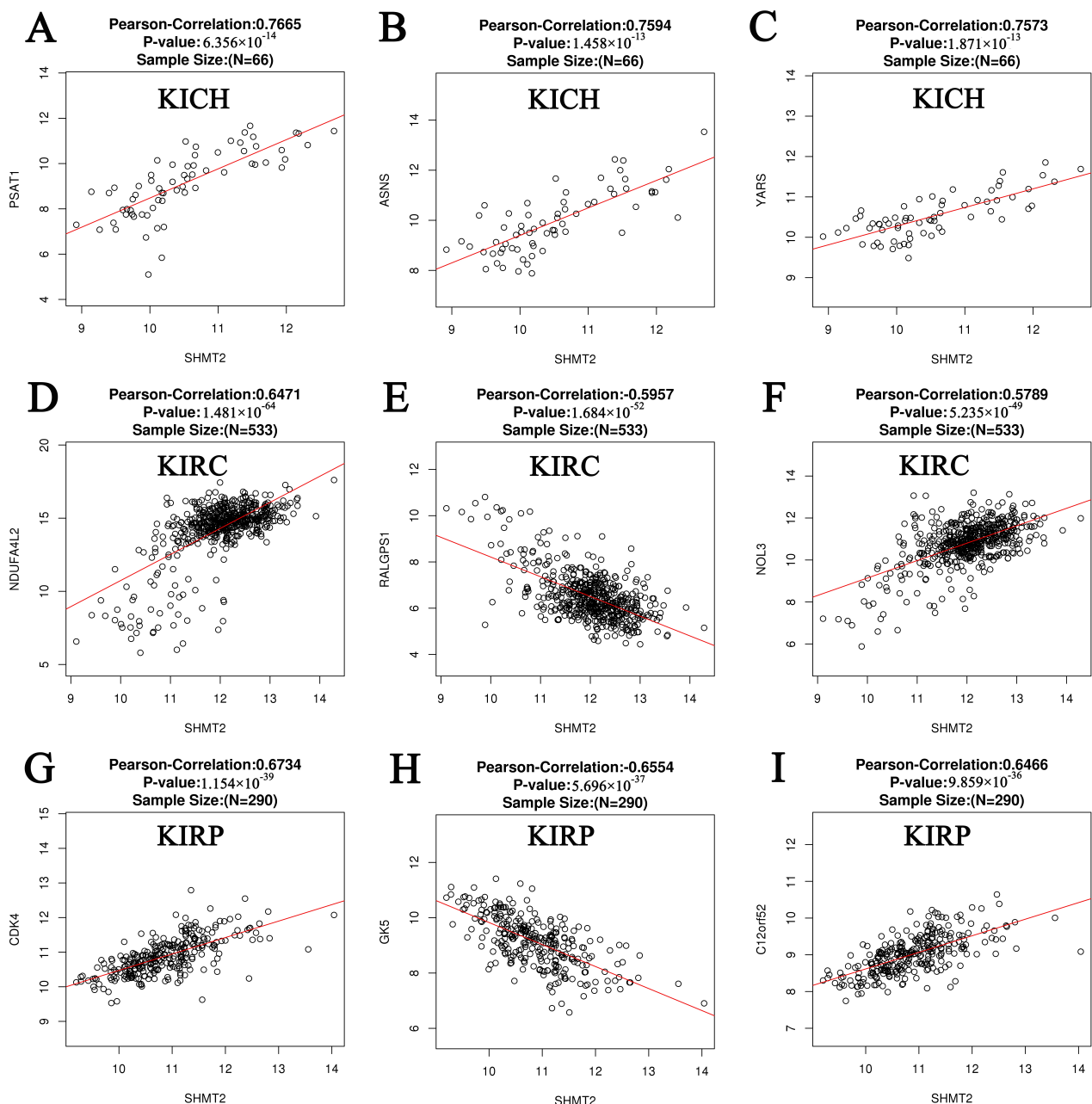


Fig. 15. Pearson correlation analysis of gene expression and *SHMT2* in RCC (LinkedOmics). (A) *PSAT1* in patients with KICH. (B) *ASNS* in patients with KICH. (C) *YARS* in patients with KICH. (D) *NDUFA4L2* in patients with KIRC. (E) *RALGAP1* in patients with KIRC. (F) *NOL3* in patients with KIRC. (G) *CDK4* in patients with KIRP. (H) *GK5* in patients with KIRP. (I) *C12orf52* in patients with KIRP.

KICH), 4% vs 4% (n = 446 patients with KIRC), and 6% vs 7% (n = 280 patients with KIRP), respectively. Moreover, *SHMT1* promoter methylation levels were significantly up-regulated in patients with KIRP. In contrast, *SHMT2* promoter methylation levels were significantly downregulated in patients with KIRC and KIRP. Genetic changes and promoter methylation often result in abnormal gene expression and function. Abnormal *SHMT1* and *SHMT2* expression caused by genetic changes and promoter methylation may

also be an essential factor. In addition, the most frequently altered NG of *SHMT1* and *SHMT2* in patients with KICH, KIRP, and KIRC were *AP5Z1*, *MUC16*, *STAG2*, *AARD*, *PAPPA2*, and *CDKN2A*. These genes promote cancer cell growth, differentiation, and invasion [24–27]. Therefore, these gene alterations may be involved, to different degrees and via different pathways, in the occurrence and development of RCC.

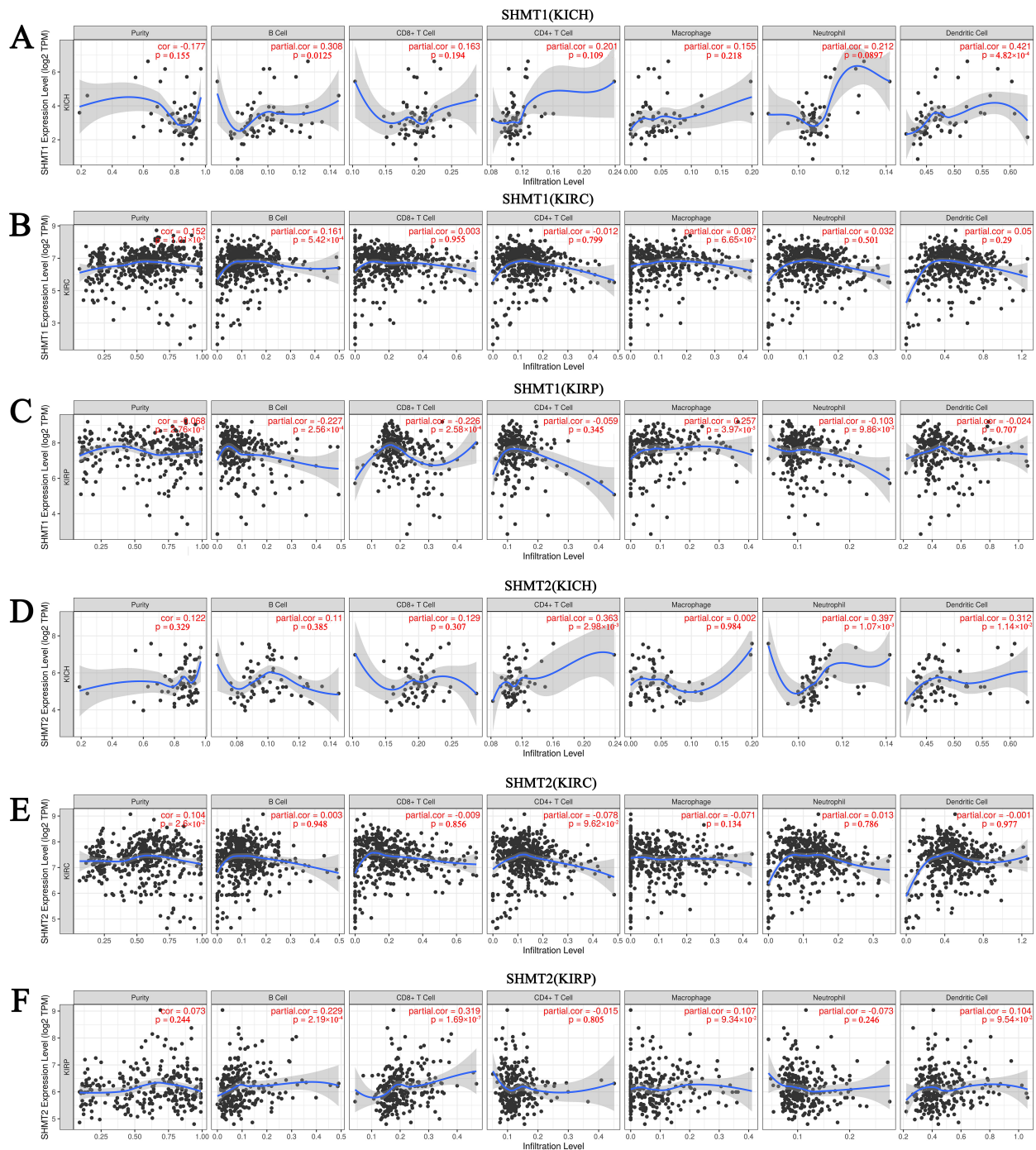


Fig. 16. Correlation between *SHMT* expression and immune cell infiltration levels in RCC (TIMER). (A) *SHMT1* in patients with KICH. (B) *SHMT1* in patients with KIRC. (C) *SHMT1* in patients with KIRP. (D) *SHMT2* in patients with KICH. (E) *SHMT2* in patients with KIRC. (F) *SHMT2* in patients with KIRP.

Finally, we assessed the prognostic value of *SHMT* expression in patients with RCC. Patients with KIRC or KIRP with high *SHMT1* expression had longer survival period than those with low *SHMT1* expression. In contrast, KICH patients with low *SHMT2* expression had longer survival period than those with high *SHMT2* expression. Interestingly, we found that patients with KIRC with high *SHMT2* expression had longer survival period than those

with low *SHMT2* expression. This contradicts the previous findings that *SHMT2* expression levels were significantly upregulated in patients with KIRC. High *SHMT2* expression may have other vital functions in patients with KIRC, which requires further investigation. In summary, *SHMT1* and *SHMT2* may be potential prognostic markers in patients with RCC.

We further evaluated the potential interactions between *SHMT* and its NG. *SHMT1*, *SHMT2*, and their NG were linked to a complex interaction network through co-expression, physical interactions, and shared protein domains. Subsequently, we evaluated the functions of *SHMT* and its NG. The molecular functions of *SHMT1* and its NG in KICH were tumor-associated metalloendopeptidase and GTPase regulatory activity. For example, membrane metalloendopeptidase inhibits prostate cancer development by attenuating the effects of gastrin-releasing peptides on stem/progenitor cells [28]. Additionally, the activation of Rap1 GTPase mediated by junctional adhesion molecule-A modulates the migration of breast cancer cells [29]. The KEGG pathway was involved in lysosome activity and endocytosis. Multidrug resistance in tumor cells reduces the efficacy of chemotherapy by preventing drug accumulation in cells through drug efflux pumps and lysosomal sequestration/exocytosis. To overcome this anti-cancer resistance, targeting lysosomes is considered an effective strategy for effective and selective anti-cancer therapy [30]. Enhancing receptor-mediated endocytosis is an essential strategy for the treatment of cancer and the reduction of side effects and multidrug resistance [31].

Furthermore, we found that active transmembrane transporter activity is related to tumor resistance, which is the molecular function of *SHMT1* and its NG among patients with KIRC [32]. The main molecular functions associated with *SHMT1* and its NG among patients with KIRP include type I interferon receptor binding, integrin binding, and protein heterodimerization related to tumor growth. Interferons are the most widely used human proteins for treating various cancers. Cell surface receptors are composed of two subunits, IFNAR1 and IFNAR2, which bind to all type I interferons and inhibit tumor growth [33]. Integrins are cell adhesion receptors (usually transmembrane glycoproteins) linked to the extracellular matrix. Enhanced integrin binding promotes cancer cell invasion and metastasis [34]. Protein heterodimerization is closely associated with tumor growth and migration. For example, HER2 and HER3, two members of the human epidermal receptor family of tyrosine kinase receptors, are associated with poor survival in patients with colorectal cancer. HER2/HER3 heterodimerization promotes the growth of colorectal cancer cells [35]. Moreover, CXCL12-CXCL4 heterodimerization prevents CXCL12-driven migration of breast cancer cells [36]. Their KEGG pathway involved the RIG-I-like receptor signaling pathway, cell cycle, and regulation of the actin cytoskeleton. Upregulation of the RIG-I-like receptor signaling pathway can promote the invasion and migration of non-small cell lung cancer cells [37]. Mitosis, the process by which cells divide, is regulated by cell cycle checkpoints. Interference with the cell cycle is vital in cancer treatment [38]. The actin cytoskeleton is an essential component of the eukaryotic cytoskeleton and plays a vital role in cancer metastasis [39].

Our results showed that the molecular functions of *SHMT2* and its NG among patients with KICH were tumor-associated cell adhesion molecule- and phospholipid binding. For example, tumor cell migration depends on the interaction between adhesion proteins and the extracellular matrix. Lutheran/basal cell adhesion molecule promotes tumor cell migration by binding to the sub-basal adhesin $\alpha 5$ chains of laminin 511 and 521 [40]. Phospholipids, major components of plasma membranes, may induce multidrug resistance and act as therapeutic targets in cancer cells [41]. In this study, protein domain-specific binding, enzyme inhibitor activity, and endopeptidase activity were the molecular functions of *SHMT2* and its NG among patients with KIRC. These functions may be necessary for cancer cell growth inhibition. Deleted-in-liver cancer 1 plays an inhibitory role in cancer growth suppression by binding to the Rho-GTPase-activating protein domain [42]. An inhibition of tartrate-resistant acid phosphatase activity can prevent the migration and invasion of breast cancer cells [43]. Asparagine endopeptidase (AEP) is highly expressed in various solid tumors and promotes cancer cells' invasion, migration, and metastasis. Blocking AEP can inhibit cancer metastasis [44]. Their KEGG pathway was involved in the cAMP and calcium signaling pathways, which are closely related to cancer development [45,46]. In addition, the molecular functions associated with *SHMT2* and its NG in patients with KIRP mainly included hormone activity, integrin binding, and protein kinase regulatory activity. These factors are closely related to the occurrence and development of RCC. Epidemiological, clinical, biochemical, and genetic studies have shown that RCC etiology is hormone-related. Hormone signaling pathways may be therapeutic targets for RCC [47].

Targeting mitogen-activated protein kinases in patients with RCC can inhibit the proliferation and migration of cancer cells [48]. Their KEGG pathway involves miRNAs in cancer. In recent years, miRNAs have become essential factors in cancer-related cachexia occurrence and participate in the mutual regulatory network of pro-inflammatory signaling pathways [49]. Hence, regulating the functions of *SHMT* and its NG may be an essential strategy for RCC treatment.

Subsequently, we explored the transcription factors and miRNA targets of *SHMT* in RCC. We found that MYC was a key transcription factor for *SHMT1* and its NG in KICH. Moreover, c-MYC promotes the growth of RCC cells by inhibiting PLA2R1 transcription [50]. Our results also showed that STAT1, which inhibits the growth of A498 RCC cells [51], was the key transcription factor of *SHMT1* and its NG in KIRC. Furthermore, we found that PPARG, NR3C1, HDAC1, STAT1, and MYC were the key transcription factors of *SHMT1* and its NG among patients with KIRP. Recent studies have shown that these transcription factors affect the progression of multiple tumors [52–54]. Furthermore, this study indicated that AR, a potential tar-

get for Xp11.2 translocation RCC therapy [55], was the key transcription factor of *SHMT2* and its NG among patients with KICH. We found that *SREBF2*, *MYCN*, and *SP3* were the key transcription factors of *SHMT2* and its NG among patients with KIRC. *SREBF2*, *MYCN*, and *SP3* regulate the proliferation and migration of multiple cancer cells [56–58]. Additionally, *FOXM1*, *DNMT1*, *REST*, and *E2F1* were the key transcription factors of *SHMT2* and its NG among patients with KIRP. These transcription factors are major drivers of tumorigenesis and progression of multiple cancers, and thus are potential targets for anti-cancer therapy [59,60]. miRNAs can be potentially use as diagnostic markers and therapeutic targets in cancer clinics. Therefore, we explored the miRNA targets of *SHMT* in patients with RCC. Recent studies have shown that these miRNAs regulate the occurrence and development of cancer. For example, miR-106 overexpression can promote proliferation and inhibit apoptosis of endometrial carcinoma RL95-2 cells [61]. Another study suggested that targeting miR-19 can inhibit the proliferation and invasion of breast cancer [62]. Moreover, miR-492 promotes cancer progression by targeting *GJB4*, a novel bladder cancer biomarker [63]. These miRNA targets are also involved in the regulation of tumor growth. For example, miR-137-3p inhibits colorectal cancer cell migration by regulating KDM1A-dependent epithelial-mesenchymal transition [64]. In addition, miR-496 inhibits the proliferation of gastric cancer cells through the AKT/mTOR signaling pathway targeting *LYN* [65]. Further, miR-493 induces the proliferation, migration, and invasion of esophageal cancer cells *in vivo* and *in vitro* by regulating the c-Jun target *Wnt5a/PD-L1* [66]. Therefore, the transcription factors and miRNA targets of *SHMT* are associated with tumor cell proliferation, migration, invasion, and drug resistance. Hence, these transcription factors and miRNA of *SHMT* may be promising targets for cancer therapy. However, their relationship with RCC has not been fully elucidated. These results suggest that the transcription factors and miRNAs of *SHMT* may be potential RCC therapeutic targets.

We examined the correlation between differentially expressed genes and *SHMT* expression in patients with RCC. We found that in patients with KICH, KIRC, and KIRP, *PRODH*, *SH3KBP1*, and *EML6*; *ACSM2B*, *ACSM2A*, and *PDZK1*; and *SMTNL2*, *ACSM2A*, and *ACSM5* were the top three genes, respectively, whose expression levels were positively associated with *SHMT1* expression. These genetic abnormalities play essential roles in the development of multiple cancers. For example, *PRODH* regulates many pathophysiological processes, including cancer cell apoptosis and metastasis [67]. A loss of *PDZK1* expression in patients with gastric cancer promotes the proliferation of gastric cancer cells by activating PI3K/AKT signaling through PTEN phosphorylation [68]. However, our results showed that in patients with KICH, KIRC, and KIRP, *PSAT1*, *ASNS*, and *YARS*; *NDUFA4L2*,

RALGPS1, and *NOL3*; and *CDK4*, *GK5*, and *C12orf52* were the top three genes, respectively, whose expression levels were positively or negatively correlated with *SHMT2* expression. These genetic abnormalities can promote multiple cancer cells' proliferation, differentiation, and metastasis. For example, *PSAT1* may act as an oncogene that plays a vital role in various cancers. *PSAT1* upregulation is involved in the growth of cervical cancer cells and cisplatin resistance via PI3K/AKT signaling pathway upregulation [69]. *NDUFA4L2* promotes trastuzumab resistance in HER2-positive breast cancer cells [70]. *CDK4* is a crucial cell cycle regulator frequently dysregulated in human malignancies. *CDK4* inhibitor use can effectively suppress tumor growth and improve the efficacy of cisplatin treatment in patients with breast and ovarian cancers [71]. Therefore, targeting these genes may serve as adjuvant therapy for RCC.

Immunotherapy is a novel clinical treatment for cancer patients. Tumor immune infiltration is closely related to clinical prognosis. As expected, *SHMT* expression in patients with RCC was positively or negatively correlated with immune cell infiltration levels. Dendritic cells are the most effective antigen-presenting cells, whereas T-cells are highly effective antitumor-effector cells. The lack of interaction between these cells is a principal mechanism of tumor tolerance [72]. B-cell infiltration plays an essential role in tumor progression and prognosis. B-cells are considered the primary effector cells involved in humoral immunity and inhibit tumor progression by secreting immunoglobulins, promoting T-cell response, and directly killing cancer cells [73]. In recent years, the complex role of neutrophils in tumorigenesis and cancer progression has attracted much attention. Neutrophils kill tumor cells through direct cytotoxic and indirect effects by activating adaptive immune responses. In contrast, the pre-tumor phenotype of neutrophils may be related to cell proliferation, angiogenesis, and immunosuppression in the tumor microenvironment. Neutrophils have recently been identified as potential targets for cancer therapy [74]. Our results showed that *SHMT1* expression was positively (B-cells and dendritic cells in KICH, B-cells in KIRC, and macrophages in KIRP) and negatively (B-cells and CD8+ T-cells in KIRP) correlated with immune cell infiltration levels. However, *SHMT2* expression was positively correlated with immune cell infiltration levels (CD4+ T-cells, neutrophils, and dendritic cells in KICH and B-cells and CD8+ T-cells in KIRP). Therefore, the aim for *SHMT* or *SHMT*-related regulatory targets may be feasible for regulating immune cell infiltration in patients with RCC.

5. Conclusions

This study systematically analyzed the expression, gene regulatory network, prognostic value, and target prediction of *SHMT* in patients with RCC. *SHMT1* and *SHMT2* expression levels were different in patients with RCC.

Therefore, different patients with RCC should be treated differently. These enzymes may be potential therapeutic and prognostic biomarkers in these patients and an essential strategy for accurately treating patients with RCC. Transcription factor regulation may be an essential strategy for RCC treatment. During this study, we successfully elucidated the relationship between *SHMT1*, *SHMT2*, and RCC and provided new insights for RCC treatment. However, further research is required to evaluate the pathological significance of the differential expression of these two *SHMT* isoenzymes in patients with RCC.

Availability of Data and Materials

The datasets used and/or analyzed during the current study are available from the corresponding author on reasonable request.

Author Contributions

YS, ZS and LD designed the research study. YS performed the research. YS, ZS, LD, JZ, WL, QL, LL, QX, JC, XL, and YC analyzed the data. All authors contributed to editorial changes in the manuscript. All authors read and approved the final manuscript. All authors have participated sufficiently in the work and agreed to be accountable for all aspects of the work.

Ethics Approval and Consent to Participate

Not applicable.

Acknowledgment

We thank Guangdong Medical University for their project support.

Funding

This work was supported by the project of financial fund science and technology special competitive allocation of Zhanjiang (Zhanke [2010]174) and postdoctoral Foundation of Guangdong Medical University (4SG22292G).

Conflict of Interest

The authors declare no conflict of interest.

References

- [1] Lobo J, Ohashi R, Amin MB, Berney DM, Comp erat EM, Cree IA, *et al.* WHO 2022 landscape of papillary and chromophobe renal cell carcinoma. *Histopathology*. 2022; 81: 426–438.
- [2] Sung H, Ferlay J, Siegel RL, Laversanne M, Soerjomataram I, Jemal A, *et al.* Global Cancer Statistics 2020: GLOBOCAN Estimates of Incidence and Mortality Worldwide for 36 Cancers in 185 Countries. *CA: A Cancer Journal for Clinicians*. 2021; 71: 209–249.
- [3] Zhang T, Gong J, Maia MC, Pal SK. Systemic Therapy for Non-Clear Cell Renal Cell Carcinoma. *American Society of Clinical Oncology Educational Book. American Society of Clinical Oncology. Annual Meeting*. 2017; 37: 337–342.
- [4] Delahunt B, Chevill e JC, Martignoni G, Humphrey PA, Magi-Galluzzi C, McKenney J, *et al.* The International Society of Urological Pathology (ISUP) grading system for renal cell carcinoma and other prognostic parameters. *The American Journal of Surgical Pathology*. 2013; 37: 1490–1504.
- [5] Liu X, Zhang M, Liu X, Sun H, Guo Z, Tang X, *et al.* Urine Metabolomics for Renal Cell Carcinoma (RCC) Prediction: Tryptophan Metabolism as an Important Pathway in RCC. *Frontiers in Oncology*. 2019; 9: 663.
- [6] Jemal A, Siegel R, Xu J, Ward E. *Cancer statistics, 2010*. *CA: A Cancer Journal for Clinicians*. 2010; 60: 277–300.
- [7] Ljungberg B, Cowan NC, Hanbury DC, Hora M, Kuczyk MA, Merseburger AS, *et al.* EAU guidelines on renal cell carcinoma: the 2010 update. *European Urology*. 2010; 58: 398–406.
- [8] Campbell SC, Novick AC, Belldegrun A, Blute ML, Chow GK, Derweesh IH, *et al.* Guideline for management of the clinical T1 renal mass. *The Journal of Urology*. 2009; 182: 1271–1279.
- [9] Hollingsworth JM, Miller DC, Daignault S, Hollenbeck BK. Five-year survival after surgical treatment for kidney cancer: a population-based competing risk analysis. *Cancer*. 2007; 109: 1763–1768.
- [10] Fujii Y, Ikeda M, Kurosawa K, Tabata M, Kamigaito T, Hosoda C, *et al.* Different clinicopathological features between patients who developed early and late recurrence following surgery for renal cell carcinoma. *International Journal of Clinical Oncology*. 2015; 20: 802–807.
- [11] Relli V, Trerotola M, Guerra E, Alberti S. Abandoning the Notion of Non-Small Cell Lung Cancer. *Trends in Molecular Medicine*. 2019; 25: 585–594.
- [12] Tramonti A, Nardella C, di Salvo ML, Barile A, Cutruzzol  F, Contestabile R. Human Cytosolic and Mitochondrial Serine Hydroxymethyltransferase Isoforms in Comparison: Full Kinetic Characterization and Substrate Inhibition Properties. *Biochemistry*. 2018; 57: 6984–6996.
- [13] Geeraerts SL, Kampen KR, Rinaldi G, Gupta P, Planque M, Louros N, *et al.* Repurposing the Antidepressant Sertraline as SHMT Inhibitor to Suppress Serine/Glycine Synthesis-Addicted Breast Tumor Growth. *Molecular Cancer Therapeutics*. 2021; 20: 50–63.
- [14] Ducker GS, Rabinowitz JD. One-Carbon Metabolism in Health and Disease. *Cell Metabolism*. 2017; 25: 27–42.
- [15] Maddocks ODK, Labuschagne CF, Adams PD, Vousden KH. Serine Metabolism Supports the Methionine Cycle and DNA/RNA Methylation through De Novo ATP Synthesis in Cancer Cells. *Molecular Cell*. 2016; 61: 210–221.
- [16] Ducker GS, Chen L, Morscher RJ, Ghergurovich JM, Esposito M, Teng X, *et al.* Reversal of Cytosolic One-Carbon Flux Compensates for Loss of the Mitochondrial Folate Pathway. *Cell Metabolism*. 2016; 23: 1140–1153.
- [17] Yang M, Vousden KH. Serine and one-carbon metabolism in cancer. *Nature Reviews. Cancer*. 2016; 16: 650–662.
- [18] Li AM, Ye J. Reprogramming of serine, glycine and one-carbon metabolism in cancer. *Biochimica et Biophysica Acta. Molecular Basis of Disease*. 2020; 1866: 165841.
- [19] Situ Y, Xu Q, Deng L, Zhu Y, Gao R, Lei L, *et al.* System analysis of *VEGFA* in renal cell carcinoma: The expression, prognosis, gene regulation network and regulation targets. *The International Journal of Biological Markers*. 2022; 37: 90–101.
- [20] Situ Y, Gao R, Lei L, Deng L, Xu Q, Shao Z. System analysis of *FHIT* in LUAD and LUSC: The expression, prognosis, gene regulation network, and regulation targets. *The International Journal of Biological Markers*. 2022; 37: 158–169.
- [21] Locasale JW. Serine, glycine and one-carbon units: cancer metabolism in full circle. *Nature Reviews. Cancer*. 2013; 13: 572–583.
- [22] Pan S, Fan M, Liu Z, Li X, Wang H. Serine, glycine and one

- carbon metabolism in cancer (Review). *International Journal of Oncology*. 2021; 58: 158–170.
- [23] García-Cañaveras JC, Lancho O, Ducker GS, Ghergurovich JM, Xu X, da Silva-Diz V, *et al.* SHMT inhibition is effective and synergizes with methotrexate in T-cell acute lymphoblastic leukemia. *Leukemia*. 2021; 35: 377–388.
- [24] Rajesh C, Sagar S, Rathinavel AK, Chemparathy DT, Peng XL, Yeh JJ, *et al.* Truncated O-Glycan-Bearing MUC16 Enhances Pancreatic Cancer Cells Aggressiveness via $\alpha 4 \beta 1$ Integrin Complexes and FAK Signaling. *International Journal of Molecular Sciences*. 2022; 23: 5459.
- [25] Gordon NS, Humayun-Zakaria N, Goel A, Abbotts B, Zeegers MP, Cheng KK, *et al.* STAG2 Protein Expression in Non-muscle-invasive Bladder Cancer: Associations with Sex, Genomic and Transcriptomic Changes, and Clinical Outcomes. *European Urology Open Science*. 2022; 38: 88–95.
- [26] Dong Y, Zhao L, Duan J, Bai H, Chen D, Li S, *et al.* PAPA2 mutation as a novel indicator stratifying beneficiaries of immune checkpoint inhibitors in skin cutaneous melanoma and non-small cell lung cancer. *Cell Proliferation*. 2022; 55: e13283.
- [27] Padhi SS, Roy S, Kar M, Saha A, Roy S, Adhya A, *et al.* Role of CDKN2A/p16 expression in the prognostication of oral squamous cell carcinoma. *Oral Oncology*. 2017; 73: 27–35.
- [28] Cheng CY, Zhou Z, Stone M, Lu B, Flesken-Nikitin A, Nanus DM, *et al.* Membrane metalloendopeptidase suppresses prostate carcinogenesis by attenuating effects of gastrin-releasing peptide on stem/progenitor cells. *Oncogenesis*. 2020; 9: 38.
- [29] McSherry EA, Brennan K, Hudson L, Hill ADK, Hopkins AM. Breast cancer cell migration is regulated through junctional adhesion molecule-A-mediated activation of Rap1 GTPase. *Breast Cancer Research*. 2011; 13: R31.
- [30] Keum C, Hong J, Kim D, Lee SY, Kim H. Lysosome-Instructioned Self-Assembly of Amino-Acid-Functionalized Perylene Diimide for Multidrug-Resistant Cancer Cells. *ACS Applied Materials & Interfaces*. 2021; 13: 14866–14874.
- [31] Tashima T. Effective cancer therapy based on selective drug delivery into cells across their membrane using receptor-mediated endocytosis. *Bioorganic & Medicinal Chemistry Letters*. 2018; 28: 3015–3024.
- [32] Puri S, Juvele K. Monocarboxylate transporter 1 and 4 inhibitors as potential therapeutics for treating solid tumours: A review with structure-activity relationship insights. *European Journal of Medicinal Chemistry*. 2020; 199: 112393.
- [33] Quadt-Akabayov SR, Chill JH, Levy R, Kessler N, Anglister J. Determination of the human type I interferon receptor binding site on human interferon- $\alpha 2$ by cross saturation and an NMR-based model of the complex. *Protein Science*. 2006; 15: 2656–2668.
- [34] Yousefi H, Vatanmakanian M, Mahdiannasser M, Mashouri L, Alahari NV, Monjezi MR, *et al.* Understanding the role of integrins in breast cancer invasion, metastasis, angiogenesis, and drug resistance. *Oncogene*. 2021; 40: 1043–1063.
- [35] Zhang BY, Zhang L, Chen YM, Qiao X, Zhao SL, Li P, *et al.* Corosolic acid inhibits colorectal cancer cells growth as a novel HER2/HER3 heterodimerization inhibitor. *British Journal of Pharmacology*. 2021; 178: 1475–1491.
- [36] Nguyen KTP, Druhan LJ, Avalos BR, Zhai L, Rauova L, Nesmelova IV, *et al.* CXCL12-CXCL4 heterodimerization prevents CXCL12-driven breast cancer cell migration. *Cellular Signalling*. 2020; 66: 109488.
- [37] Tang XD, Zhang DD, Jia L, Ji W, Zhao YS. lncRNA AFAP1-AS1 Promotes Migration and Invasion of Non-Small Cell Lung Cancer via Up-Regulating IRF7 and the RIG-I-Like Receptor Signaling Pathway. *Cellular Physiology and Biochemistry*. 2018; 50: 179–195.
- [38] Vakili-Samiani S, Khanghah OJ, Gholipour E, Najafi F, Zeinalzadeh E, Samadi P, *et al.* Cell cycle involvement in cancer therapy; WEE1 kinase, a potential target as therapeutic strategy. *Mutation Research*. 2022; 824: 111776.
- [39] Ma X, Dang Y, Shao X, Chen X, Wu F, Li Y. Ubiquitination and Long Non-coding RNAs Regulate Actin Cytoskeleton Regulators in Cancer Progression. *International Journal of Molecular Sciences*. 2019; 20: 2997.
- [40] Guadall A, Cochet S, Renaud O, Colin Y, Le Van Kim C, de Brevern AG, *et al.* Dimerization and phosphorylation of Lutheran/basal cell adhesion molecule are critical for its function in cell migration on laminin. *The Journal of Biological Chemistry*. 2019; 294: 14911–14921.
- [41] Kopecka J, Trouillas P, Gašparović AČ, Gazzano E, Assaraf YG, Riganti C. Phospholipids and cholesterol: Inducers of cancer multidrug resistance and therapeutic targets. *Drug Resistance Updates*. 2020; 49: 100670.
- [42] Joshi R, Qin L, Cao X, Zhong S, Voss C, Min W, *et al.* DLC1 SAM domain-binding peptides inhibit cancer cell growth and migration by inactivating RhoA. *The Journal of Biological Chemistry*. 2020; 295: 645–656.
- [43] Krumpel M, Reithmeier A, Senge T, Baeumler TA, Frank M, Nyholm PG, *et al.* The small chemical enzyme inhibitor 5-phenylpicotinic acid/CD13 inhibits cell migration and invasion of tartrate-resistant acid phosphatase/ACP5-overexpressing MDA-MB-231 breast cancer cells. *Experimental Cell Research*. 2015; 339: 154–162.
- [44] Qi Q, Obiany O, Du Y, Fu H, Li S, Ye K. Blockade of Asparagine Endopeptidase Inhibits Cancer Metastasis. *Journal of Medicinal Chemistry*. 2017; 60: 7244–7255.
- [45] Ahmed MB, Alghamdi AAA, Islam SU, Lee JS, Lee YS. cAMP Signaling in Cancer: A PKA-CREB and EPAC-Centric Approach. *Cells*. 2022; 11: 2020.
- [46] Wang XX, Xiao FH, Li QG, Liu J, He YH, Kong QP. Large-scale DNA methylation expression analysis across 12 solid cancers reveals hypermethylation in the calcium-signaling pathway. *Oncotarget*. 2017; 8: 11868–11876.
- [47] Czarnecka AM, Niedzwiedzka M, Porta C, Szczylik C. Hormone signaling pathways as treatment targets in renal cell cancer (Review). *International Journal of Oncology*. 2016; 48: 2221–2235.
- [48] Su Z, Chen D, Zhang E, Li Y, Yu Z, Shi M, *et al.* MicroRNA-509-3p inhibits cancer cell proliferation and migration by targeting the mitogen-activated protein kinase kinase kinase 8 oncogene in renal cell carcinoma. *Molecular Medicine Reports*. 2015; 12: 1535–1543.
- [49] Santos JMO, Peixoto da Silva S, Bastos MMSM, Oliveira PA, Gil da Costa RM, Medeiros R. Decoding the role of inflammation-related microRNAs in cancer cachexia: a study using HPV16-transgenic mice and *in silico* approaches. *Journal of Physiology and Biochemistry*. 2022; 78: 439–455.
- [50] Vindrieux D, Devailly G, Augert A, Le Calvé B, Ferrand M, Pigny P, *et al.* Repression of PLA2R1 by c-MYC and HIF-2 α promotes cancer growth. *Oncotarget*. 2014; 5: 1004–1013.
- [51] Zhang F, Shang D, Zhang Y, Tian Y. Interleukin-22 suppresses the growth of A498 renal cell carcinoma cells via regulation of STAT1 pathway. *PLoS ONE*. 2011; 6: e20382.
- [52] Ding X, Han X, Yuan H, Zhang Y, Gao Y. The Impact of PPAR α and PPAR γ Polymorphisms on Glioma Risk and Prognosis. *Scientific Reports*. 2020; 10: 5140.
- [53] Xiong H, Chen Z, Lin B, Xie B, Liu X, Chen C, *et al.* Naringenin Regulates FKBP4/NR3C1/NRF2 Axis in Autophagy and Proliferation of Breast Cancer and Differentiation and Maturation of Dendritic Cell. *Frontiers in Immunology*. 2022; 12: 745111.
- [54] Xu Y, Feng Y, Sun Z, Li Q. RNF168 promotes RHOc degradation by ubiquitination to restrain gastric cancer progression via decreasing HDAC1 expression. *Biochemical and Biophysical*

- cal Research Communications. 2021; 557: 135–142.
- [55] Liu N, Chen Y, Yang L, Shi Q, Lu Y, Ma W, *et al.* Both SUMOylation and ubiquitination of TFE3 fusion protein regulated by androgen receptor are the potential target in the therapy of Xp11.2 translocation renal cell carcinoma. *Clinical and Translational Medicine*. 2022; 12: e797.
- [56] Cai C, Zhang Y, Peng X. Knocking down Sterol regulatory element binding protein 2 (SREBF2) inhibits the Serine Protease 8 (PRSS8) /sodium channel epithelial 1alpha subunit (SCNN1A) axis to reduce the cell proliferation, migration and epithelial-mesenchymal transformation of ovarian cancer. *Bioengineered*. 2021; 12: 9390–9400.
- [57] Shen Z, Sun S. CircPTCH1 Promotes Migration in Lung Cancer by Regulating MYCN Expression Through miR-34c-5p. *Oncotargets and Therapy*. 2021; 14: 4779–4789.
- [58] Mansour MA. SP3 is associated with migration, invasion, and Akt/PKB signalling in MDA-MB-231 breast cancer cells. *Journal of Biochemical and Molecular Toxicology*. 2021; 35: e22657.
- [59] Wang K, Dai X, Yu A, Feng C, Liu K, Huang L. Peptide-based PROTAC degrader of FOXM1 suppresses cancer and decreases GLUT1 and PD-L1 expression. *Journal of Experimental & Clinical Cancer Research*. 2022; 41: 289.
- [60] Ma X, Li Y, Zhao B. Ribosomal protein L5 (RPL5)/ E2F transcription factor 1 (E2F1) signaling suppresses breast cancer progression via regulating endoplasmic reticulum stress and autophagy. *Bioengineered*. 2022; 13: 8076–8086.
- [61] Li X, Yi X, Bie C, Wang Z. Expression of miR-106 in endometrial carcinoma RL95-2 cells and effect on proliferation and invasion of cancer cells. *Oncology Letters*. 2018; 16: 2251–2254.
- [62] Liu AX, Yang F, Huang L, Zhang LY, Zhang JR, Zheng RN. Long non-coding RNA Tubulin Alpha 4B (TUBA4B) inhibited breast cancer proliferation and invasion by directly targeting miR-19. *European Review for Medical and Pharmacological Sciences*. 2019; 23: 708–715.
- [63] Wang K, Lü H, Qu H, Xie Q, Sun T, Gan O, *et al.* miR-492 Promotes Cancer Progression by Targeting GJB4 and Is a Novel Biomarker for Bladder Cancer. *Oncotargets and Therapy*. 2019; 12: 11453–11464.
- [64] Ding X, Zhang J, Feng Z, Tang Q, Zhou X. MiR-137-3p Inhibits Colorectal Cancer Cell Migration by Regulating a KDM1A-Dependent Epithelial-Mesenchymal Transition. *Digestive Diseases and Sciences*. 2021; 66: 2272–2282.
- [65] Su R, Zhao E, Zhang J. miR-496 inhibits proliferation via LYN and AKT pathway in gastric cancer. *Open Medicine*. 2021; 16: 1206–1214.
- [66] Bian W, Li Y, Zhu H, Gao S, Niu R, Wang C, *et al.* miR-493 by regulating of c-Jun targets Wnt5a/PD-L1-inducing esophageal cancer cell development. *Thoracic Cancer*. 2021; 12: 1579–1588.
- [67] Liu Y, Mao C, Liu S, Xiao D, Shi Y, Tao Y. Proline dehydrogenase in cancer: apoptosis, autophagy, nutrient dependency and cancer therapy. *Amino Acids*. 2021; 53: 1891–1902.
- [68] Zhao C, Tao T, Yang L, Qin Q, Wang Y, Liu H, *et al.* Loss of PDZK1 expression activates PI3K/AKT signaling via PTEN phosphorylation in gastric cancer. *Cancer Letters*. 2019; 453: 107–121.
- [69] Duan W, Liu X. PSAT1 Upregulation Contributes to Cell Growth and Cisplatin Resistance in Cervical Cancer Cells via Regulating PI3K/AKT Signaling Pathway. *Annals of Clinical and Laboratory Science*. 2020; 50: 512–518.
- [70] Yuan Y, Gao H, Zhuang Y, Wei L, Yu J, Zhang Z, *et al.* NDUFA4L2 promotes trastuzumab resistance in HER2-positive breast cancer. *Therapeutic Advances in Medical Oncology*. 2021; 13: 17588359211027836.
- [71] Tian C, Wei Y, Li J, Huang Z, Wang Q, Lin Y, *et al.* A Novel CDK4/6 and PARP Dual Inhibitor ZC-22 Effectively Suppresses Tumor Growth and Improves the Response to Cisplatin Treatment in Breast and Ovarian Cancer. *International Journal of Molecular Sciences*. 2022; 23: 2892.
- [72] Lurje I, Hammerich L, Tacke F. Dendritic Cell and T Cell Crosstalk in Liver Fibrogenesis and Hepatocarcinogenesis: Implications for Prevention and Therapy of Liver Cancer. *International Journal of Molecular Sciences*. 2020; 21: 7378.
- [73] Tokunaga R, Naseem M, Lo JH, Battaglin F, Soni S, Puccini A, *et al.* B cell and B cell-related pathways for novel cancer treatments. *Cancer Treatment Reviews*. 2019; 73: 10–19.
- [74] Que H, Fu Q, Lan T, Tian X, Wei X. Tumor-associated neutrophils and neutrophil-targeted cancer therapies. *Biochimica et Biophysica Acta. Reviews on Cancer*. 2022; 1877: 188762.